Drell-Yan as a probe of the nucleus

Hyunchul Kim 김현철
(Chonnam National University)

The 10th ATHIC 2025
January 14, 2025
Mayfair Palm Beach Resort, Gopalpur-On-Sea,
Berhampur, Odisha, India

What is the Drell-Yan (DY) process?

- **In 1970, Sidney Drell and Tung-Mow Yan suggested to explain the production of lepton-antilepton pairs in high-energy collisions**

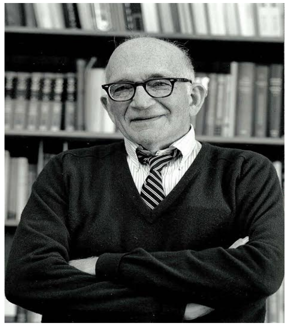

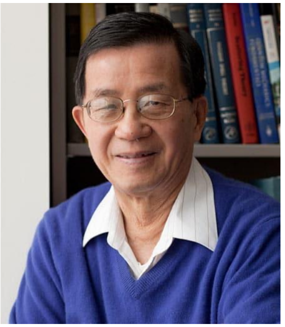

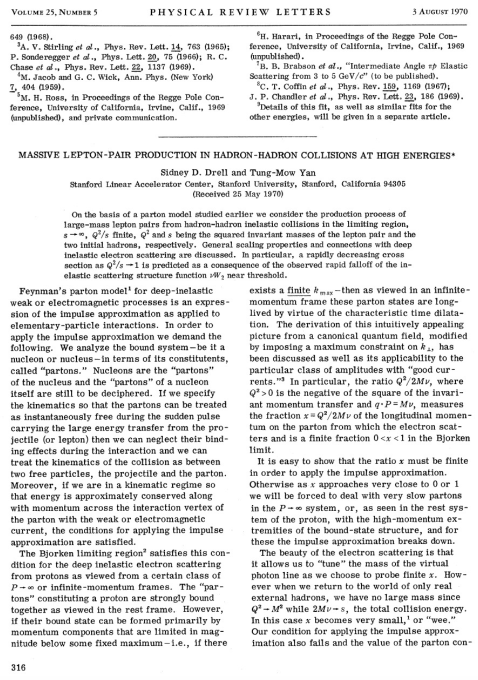

VOLUME 25, NUMBER 5 PHYSICAL REVIEW LETTERS 3 AUGUST 1970

649 (1968).
[3]A. V. Stirling *et al.*, Phys. Rev. Lett. 14, 763 (1965); P. Sonderegger *et al.*, Phys. Lett. 20, 75 (1966); R. C. Chase *et al.*, Phys. Rev. Lett. 22, 1137 (1969).
[4]M. Jacob and G. C. Wick, Ann. Phys. (New York) 7, 404 (1959).
[5]M. H. Ross, in Proceedings of the Regge Pole Conference, University of California, Irvine, Calif., 1969 (unpublished), and private communication.
[6]H. Harari, in Proceedings of the Regge Pole Conference, University of California, Irvine, Calif., 1969 (unpublished).
[7]B. B. Brabson *et al.*, "Intermediate Angle πp Elastic Scattering from 3 to 5 GeV/c" (to be published).
[8]C. T. Coffin *et al.*, Phys. Rev. 159, 1169 (1967); J. P. Chandler *et al.*, Phys. Rev. Lett. 23, 186 (1969).
[9]Details of this fit, as well as similar fits for the other energies, will be given in a separate article.

MASSIVE LEPTON-PAIR PRODUCTION IN HADRON-HADRON COLLISIONS AT HIGH ENERGIES*

Sidney D. Drell and Tung-Mow Yan
Stanford Linear Accelerator Center, Stanford University, Stanford, California 94305
(Received 25 May 1970)

On the basis of a parton model studied earlier we consider the production process of large-mass lepton pairs from hadron-hadron inelastic collisions in the limiting region, $s \to \infty$, Q^2/s finite, Q^2 and s being the squared invariant masses of the lepton pair and the two initial hadrons, respectively. General scaling properties and connections with deep inelastic electron scattering are discussed. In particular, a rapidly decreasing cross section as $Q^2/s \to 1$ is predicted as a consequence of the observed rapid falloff of the inelastic scattering structure function νW_2 near threshold.

Feynman's parton model[1] for deep-inelastic weak or electromagnetic processes is an expression of the impulse approximation as applied to elementary-particle interactions. In order to apply the impulse approximation we demand the following. We analyze the bound system—be it a nucleon or nucleus—in terms of its constitutents, called "partons." Nucleons are the "partons" of the nucleus and the "partons" of a nucleon itself are still to be deciphered. If we specify the kinematics so that the partons can be treated as instantaneously free during the sudden pulse carrying the large energy transfer from the projectile (or lepton) then we can neglect their binding effects during the interaction and we can treat the kinematics of the collision as between two free particles, the projectile and the parton. Moreover, if we are in a kinematic regime so that energy is approximately conserved along with momentum across the interaction vertex of the parton with the weak or electromagnetic current, the conditions for applying the impulse approximation are satisfied.

The Bjorken limiting region[2] satisfies this condition for the deep inelastic electron scattering from protons as viewed from a certain class of $P \to \infty$ or infinite-momentum frames. The "partons" constituting a proton are strongly bound together as viewed in the rest frame. However, if their bound state can be formed primarily by momentum components that are limited in magnitude below some fixed maximum—i.e., if there exists a finite k_{max}—then as viewed in an infinite-momentum frame these parton states are long-lived by virtue of the characteristic time dilatation. The derivation of this intuitively appealing picture from a canonical quantum field, modified by imposing a maximum constraint on $k_\perp$, has been discussed as well as its applicability to the particular class of amplitudes with "good currents."[3] In particular, the ratio $Q^2/2M\nu$, where $Q^2 > 0$ is the negative of the square of the invariant momentum transfer and $q \cdot P = M\nu$, measures the fraction $x \equiv Q^2/2M\nu$ of the longitudinal momentum on the parton from which the electron scatters and is a finite fraction $0 < x < 1$ in the Bjorken limit.

It is easy to show that the ratio x must be finite in order to apply the impulse approximation. Otherwise as x approaches very close to 0 or 1 we will be forced to deal with very slow partons in the $P \to \infty$ system, or, as seen in the rest system of the proton, with the high-momentum extremities of the bound-state structure, and for these the impulse approximation breaks down.

The beauty of the electron scattering is that it allows us to "tune" the mass of the virtual photon line as we choose to probe finite x. However when we return to the world of only real external hadrons, we have no large mass since $Q^2 \to M^2$ while $2M\nu \to s$, the total collision energy. In this case x becomes very small,[1] or "wee." Our condition for applying the impulse approximation also fails and the value of the parton con-

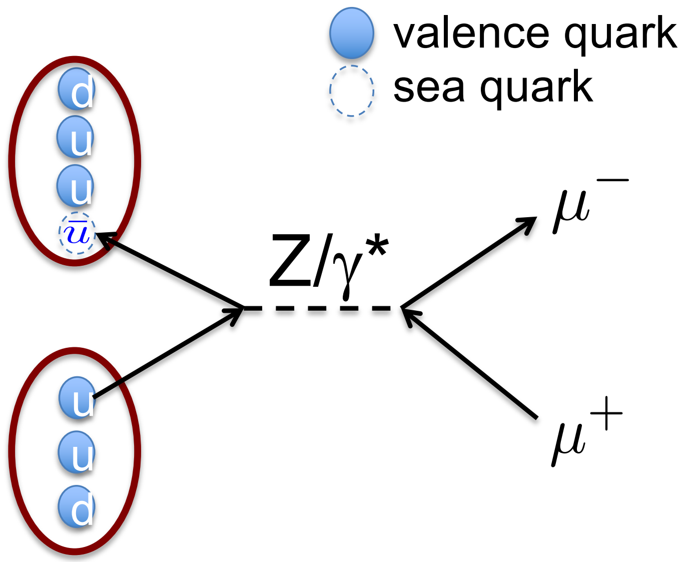

Annihilation of quark-antiquark

Via Z boson or virtual γ

Decay to dilepton (muon, electron)

Phys. Rev. Lett. **25**, 316 (1970)
Erratum Phys. Rev. Lett. **25**, 902 (1970)

Parton Distribution Function (PDF) and nuclear PDF(nPDF)

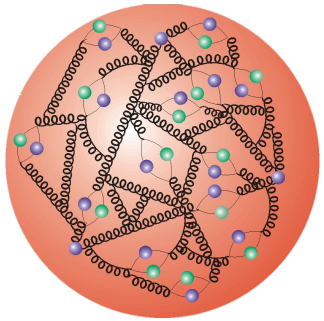

CT18 NNLO PDF

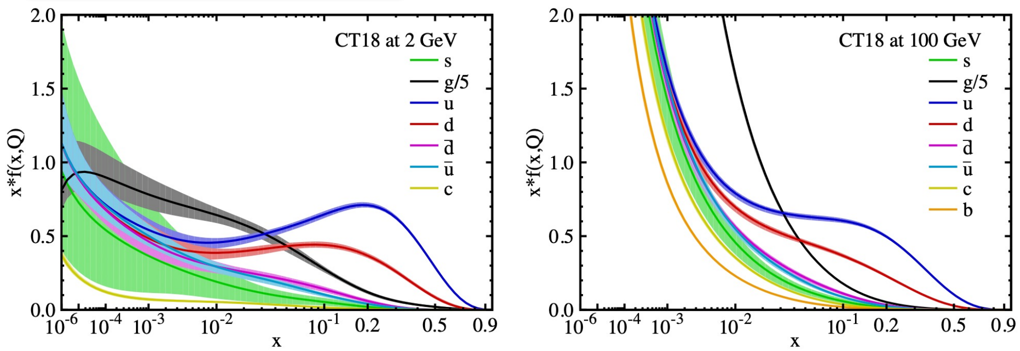

x : momentum fraction of parton
Q^2 : scale of scattering

PRD 103 (2021) 014013

- **Probability density for finding a parton within the proton**
  - Flavor, momentum fraction, scale of scattering dependence

$$x = \frac{Q}{\sqrt{s_{\mathrm{NN}}}} e^{y_{\mathrm{CM}}}$$

- **x : momentum fraction**
- **Q : dimuon mass**
- $\sqrt{s_{NN}}$: collision energy
- y_{CM} : dimuon's rapidity in center-of-mass frame

Parton Distribution Function (PDF) and nuclear PDF(nPDF)

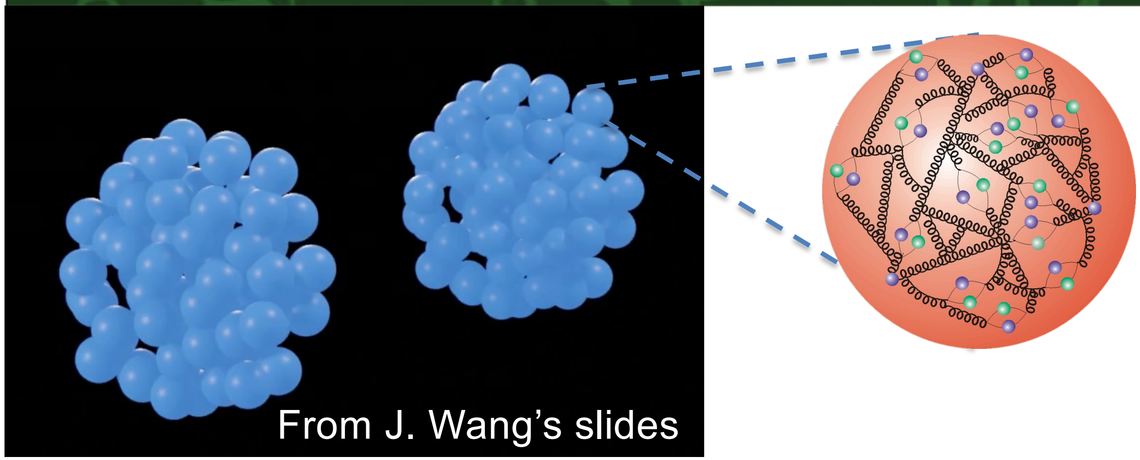

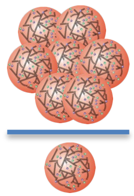

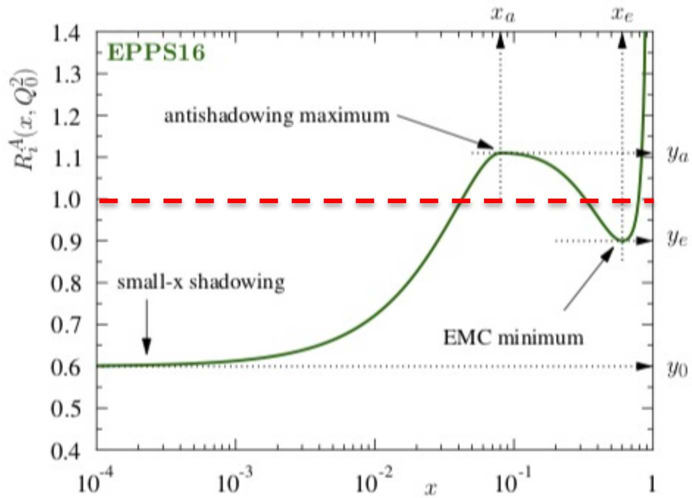

- **Probability density for finding a parton within the proton**
  - Flavor, momentum fraction, scale of scattering dependence
- **nPDF : modified parton distribution function in the bound nucleons**

List of some nPDFs

	nCTEQ15HQ	EPPS21	nNNPDF3.0	TUJU21	KSASG20
Order in α_s	**NLO**	**NLO**	**NLO**	**NNLO**	**NNLO**
DIS lA	✓	✓	✓	✓	✓
Drell-Yan pA	✓	✓	✓		✓
Drell-Yan πA		✓	✓		
LHC pPb dijets		✓	✓		
LHC pPb W & Z	✓	✓	✓	✓	✓
LHC pPb D-mesons	✓	✓	✓		
RHIC dAu π^0, $\pi^\pm$	✓	✓			✓
Baseline proton PDF	**~CTEQ6.1**	**CT18A**	**~NNPDF4.0**	**~HERAPDF2.0**	**CT18**
Data points	1484	2077	2188	2410	4353
Free parameters	19	24	256	16	18
Error analysis	Hessian	Hessian	Monte Carlo	Hessian	Hessian
Reference	PRD 105 (2022) 114043	EPJC 82 (2022) 413	arXiv (2022) 2201.12363	arXiv (2022) 2207.04654	PRD 104 (2021) 034010

Based on Ann. Rev. Nucl. Part. Sci. 2024 74:1-41

List of some nPDFs

	nCTEQ15HQ	EPPS21	nNNPDF3.0	TUJU21	KSASG20
Order in α_s	NLO	NLO	NLO	NNLO	NNLO
DIS lA	✓	✓	✓	✓	✓
Drell-Yan pA	✓	✓	✓		✓
Drell-Yan πA					
LHC pPb dije					
LHC pPb W					✓
LHC pPb D-m					
RHIC dAu π^0, π					✓
Baseline proto					CT18
Data points					4353
Free parameters					18
Error analysis					Hessian
Reference	PRD 105 (2022) 114043	EPJC 82 (2022) 413	arXiv (2022) 2201.12363	arXiv (2022) 2207.04654	PRD 104 (2021) 034010

Various nPDFs in Pb nucleus

arXiv:2112.12462

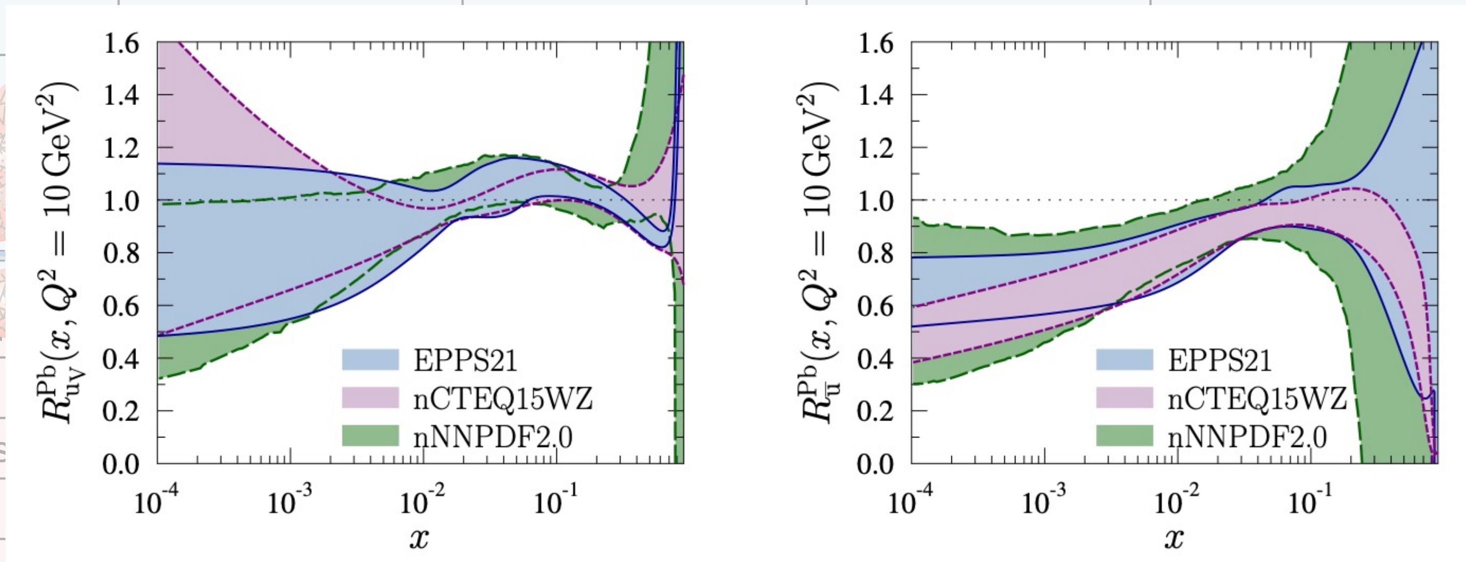

Based on Ann. Rev. Nucl. Part. Sci. 2024 74:1-41

We have another probes – Electroweak probes

- **Condition of the probe for initial stages**
  - Information with initial stages
  - No final state interaction with QCD matter after the collisions
    → No color charge

- **Electroweak probes**
  - W boson
    - $u\bar{d} \rightarrow W^{+}, d\bar{u} \rightarrow W^{-}$
    - By decay lepton and neutrino measured by missing E_T
    - Charge asymmetry could be useful
  - Prompt photons — In detail, Roli's talk
    - Not decayed from hadrons
    - Sensitive to gluon distributions

W boson

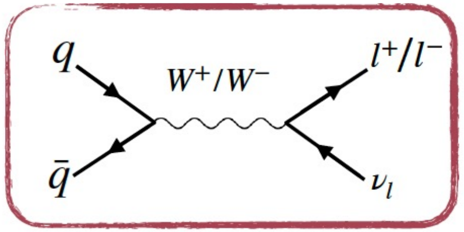

Prompt photons

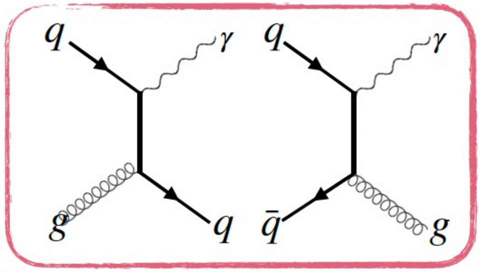

qg Compton scattering   qq̄ annihilation

Drell-Yan process

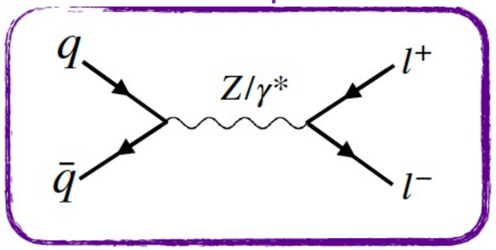

Why DY is more powerful?

- **Features of the Drell-Yan process**
  - Direct connection of PDFs
  - Theoretical Simplicity
  - Broad x and Q^2 coverage

- **Electroweak probes**
  - W boson
    - Decayed neutrinos make larger uncertainties in reconstructing missing energy
    - Less sensitive to low x and Q^2 regions
  - Prompt photons
    - Significant background contamination
    - More complex theoretical predictions due to higher-order QCD corrections, increasing uncertainties

W boson

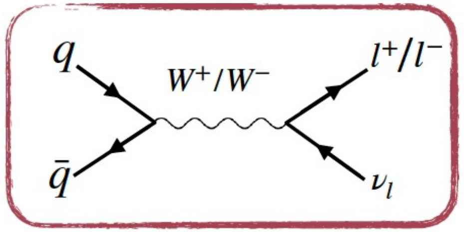

Prompt photons

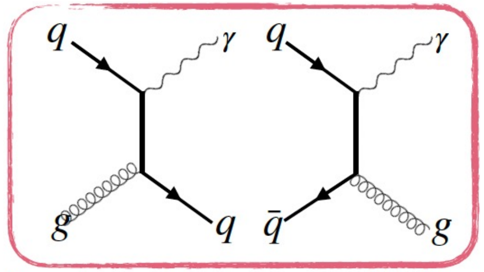

qg Compton scattering $q\bar{q}$ annihilation

Drell-Yan process

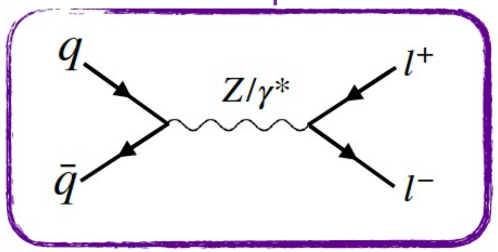

History of DY, Z boson measurement in ion collision

	pPb	PbPb
CMS	PLB 759 (2016) 36 : Differential cross section, R_{FB} JHEP 05 (2021) 182 : DY, Differential cross section, R_{FB}	PRL 106 (2011) 212301 : Differential cross section JHEP 03 (2015) 022 : Differential cross section, R_{AA} PRL 127 (2021) 102002 : T_{AA}-normalized Z boson yields PRL 128 (2022) 122301 : angular dependence
ATLAS	PRC 92 (2015) 044915 : Differential cross section	PLB 697 (2011) 294 : Z boson reconstruction PRL 110 (2013) 022301 : Differential cross section, v_2 PLB 802 (2020) 135262 : Differential cross section, R_{AA}
ALICE	JHEP 02 (2017) 077 : Production cross section (mainly W boson) JHEP 2009 (2020) 076 : Differential cross section	PLB 780 (2018) 372 : Differential cross section, R_{AA} JHEP 2009 (2020) 076 : Differential cross section, R_{AA}
LHCb	JHEP 09 (2014) 030 : Differential cross section JHEP 06 (2023) 022 : Differential cross section, R_{FB}, R_{pPb}	

Reconstruction of Z boson

- **Reconstruct with dimuon or dielectron pair**
- **Clean signal with good signal to background ratio (S/B)**
  - Even if 38-39 Z boson and publish first series of paper from Z boson at LHC

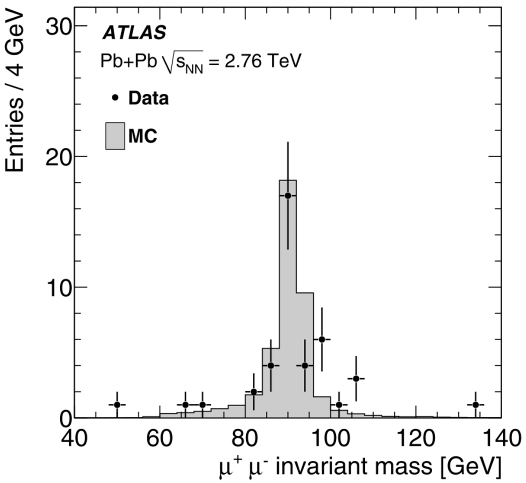

ATLAS : PLB 697 (2011) 294
2.76 TeV PbPb, 6.7 μb^{-1}

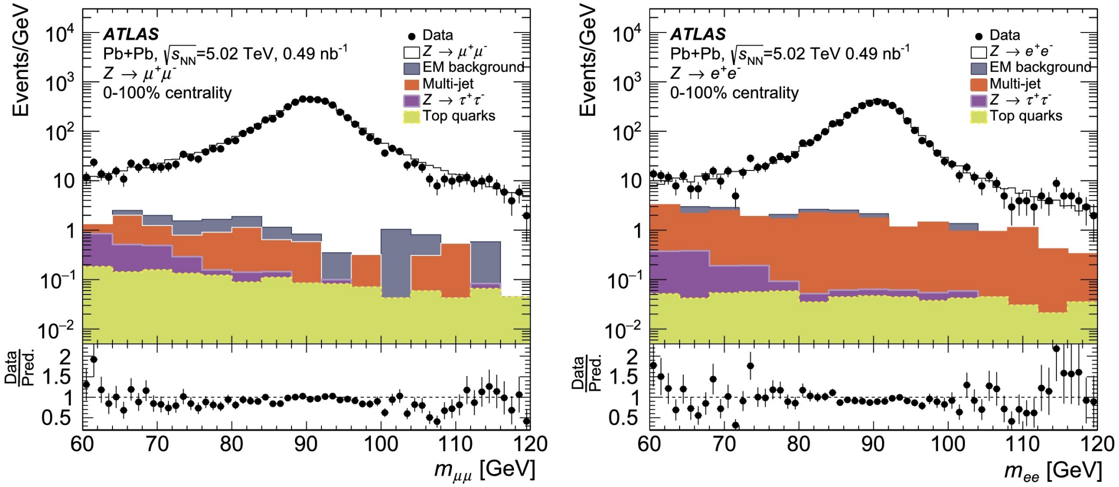

ATLAS : PLB 802 (2020) 135262
5.02 TeV PbPb, 490 μb^{-1}

Previous Z boson measurement – in the sight of PDF and nPDF

- Compared to proton PDF and nPDF with same proton PDF as the baseline
- In AA collision, not distinguish favor between proton PDF and nPDF

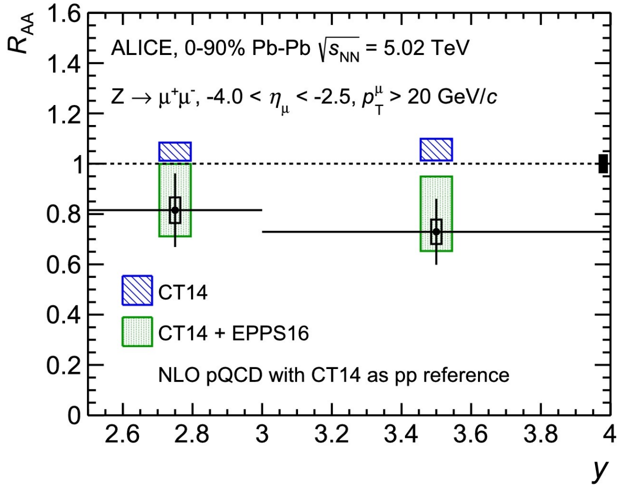

ALICE : PLB 780 (2018) 372

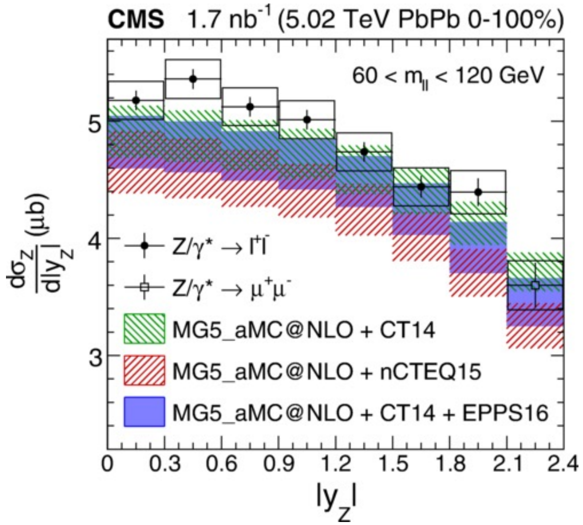

CMS : PRL 127 (2021) 102002

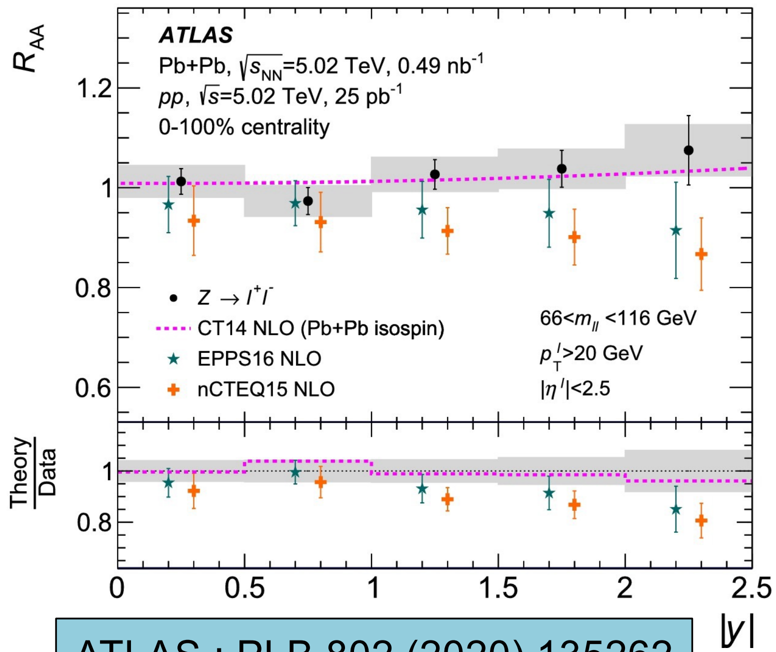

ATLAS : PLB 802 (2020) 135262

Previous Z boson measurement – in the sight of PDF and nPDF

- **Compared to proton PDF and nPDF with same proton PDF as the baseline**
- **In AA collision, not distinguish favor between proton PDF and nPDF**
- **In pA collision, nPDF is favor to the proton PDF**

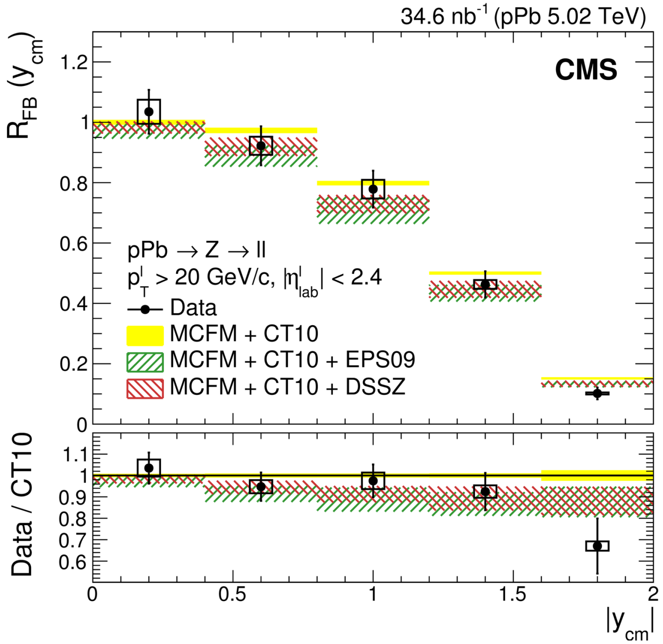

CMS : PLB 759 (2016) 36

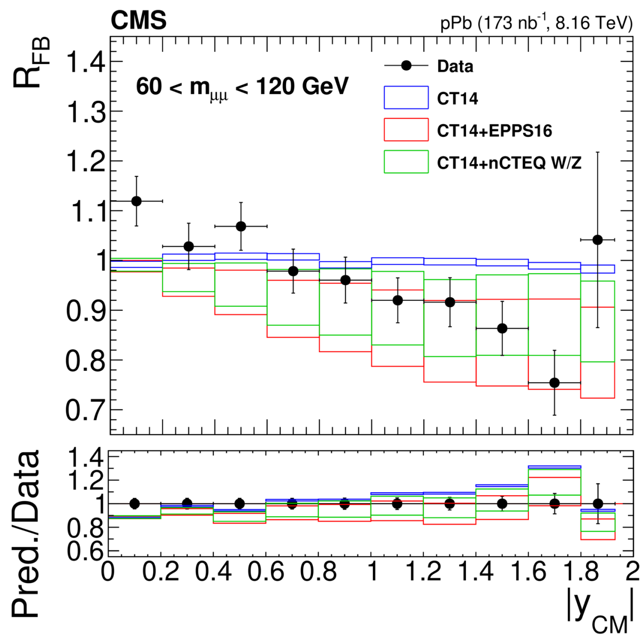

CMS : JHEP 05 (2021) 182

Now from LHC, we only have one DY result in ion collision..

- **Should be the reference and need to focus here**
- **First trial of the DY analysis in 8.16 TeV pPb collision** JHEP 05 (2021) 182
  - pPb collision can access smaller x than PbPb or pp collisions
  - Expect smaller QCD backgrounds than in PbPb
- **Summary of the condition**
  - Total integrated luminosity : 173.4 ± 6.1 nb^{-1}
  - Trigger : Require at least one muon with $p_T > 15$ GeV
  - Kinematic cuts with offline reconstructed muons
    - At least two muons with opposite charges
    - $|\eta_{lab}| < 2.4$: CMS muon acceptance
    - $p_T > 10$ GeV (at least one with $p_T > 15$ GeV)

$$x = \frac{Q}{\sqrt{s_{NN}}} e^{y_{CM}}$$

- x : momentum fraction
- Q : dimuon mass
- $\sqrt{s_{NN}}$: collision energy
- y_{CM} : dimuon's rapidity in center-of-mass frame

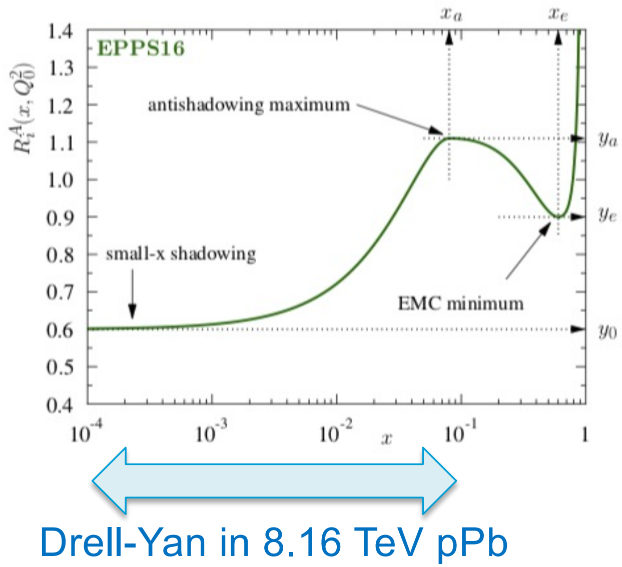

Measured variables in proton-ion collisions

- **Cross sections**
  - Wide mass coverage 15-600 GeV

Cross section	$15 < M_{\mu\mu} < 60$ GeV	$60 < M_{\mu\mu} < 120$ GeV
vs. p_T	First measurement	Highest precision
vs. $\lvert y \rvert$ (y : -2.87~1.93)	First measurement	Highest precision
vs. ϕ^*	First measurement	First measurement

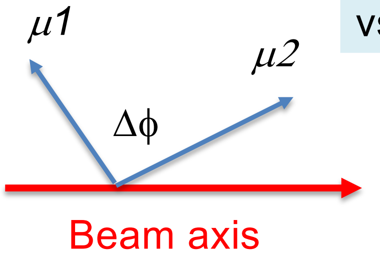

opening angle between the leptons

$$\phi^* \equiv \tan\left(\frac{\pi - \Delta\phi}{2}\right)\sin(\theta^*_\eta), \quad \cos(\theta^*_\eta) = \tanh(\Delta\eta/2)$$

related to the emission angle of the dilepton system with respect to the beam

- ϕ^* ~ **dimuon p_T** / dimuon mass
- Better precision than p_T especially at lower p_T values
- $\phi^* < 1$ corresponds to dimuon p_T up to 100 GeV near the Z boson peak

- **Forward-backward ratios (R_{FB})**

p-going y>0

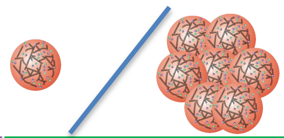

Pb-going y<0

	$15 < M_{\mu\mu} < 60$ GeV	$60 < M_{\mu\mu} < 120$ GeV
R_{FB}	First measurement	Highest precision

Background estimation (key point)

- **Various kinds of background source**

- **Involving two isolated muons**
  - t, W related : Z/γ^* $\rightarrow$ $\tau^+\tau^-$, ttbar, tW, dibosons
    - Estimated from simulation and corrected using the "eμ method"
  - The small contribution from heavy-flavor meson decays is estimated from same-sign eμ events

- **With one or more muons in jets (W+ jets and multijet)**
  - Estimated by the "misidentification rate method"

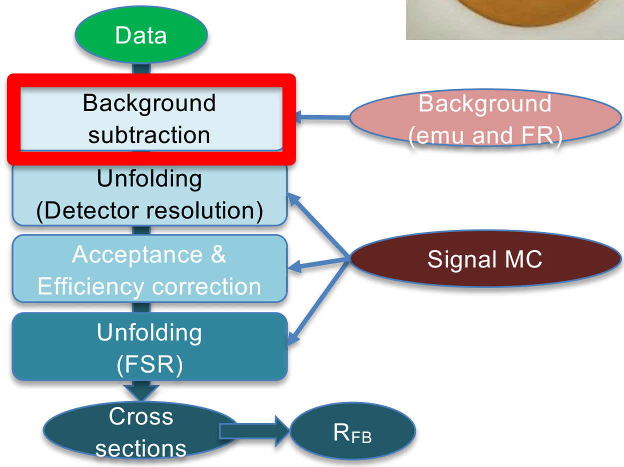

Condition for EW related MC
- Using the NLO generator POWHEG v2
- **CT14 + EPPS16 nPDF** is used
- Parton showering by PYTHIA 8.212 with the CUETP8M1 underlying event tune

Diboson and QCD multijet, and signal MC
- Leading order using PYTHIA

Comparison of the data with signal and background

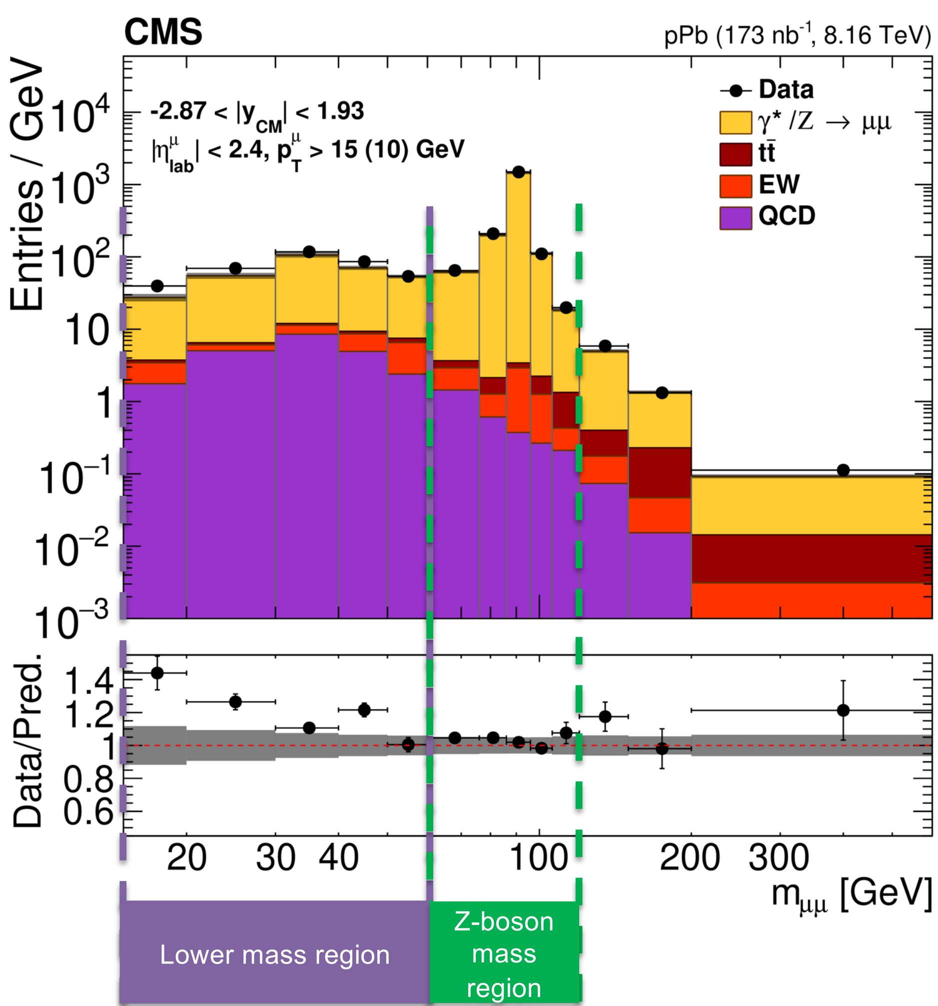

Lower mass region
$15 < m_{\mu\mu} < 60$ GeV

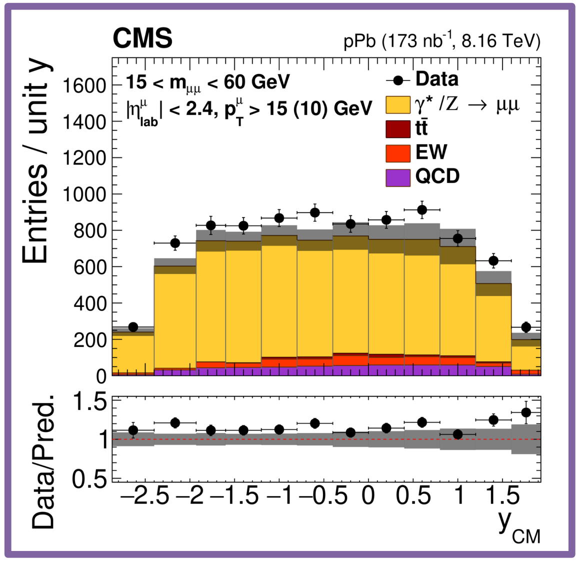

Z-boson mass region
$60 < m_{\mu\mu} < 120$ GeV

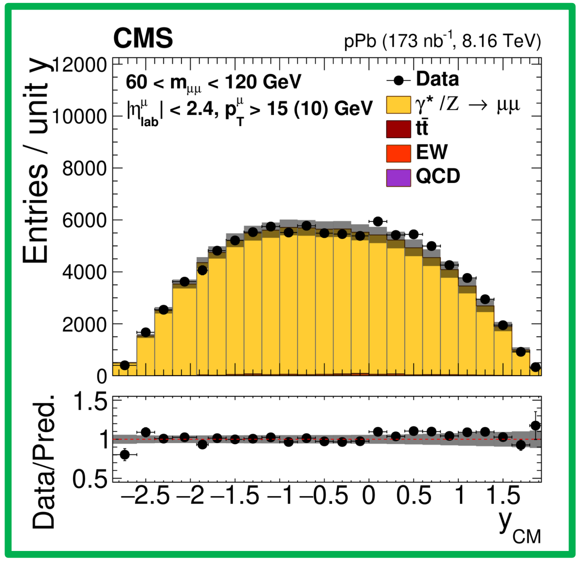

- **A good overall agreement between data and prediction, which is dominated by DY signal**

Differential cross sections

Corrected with acceptance correction

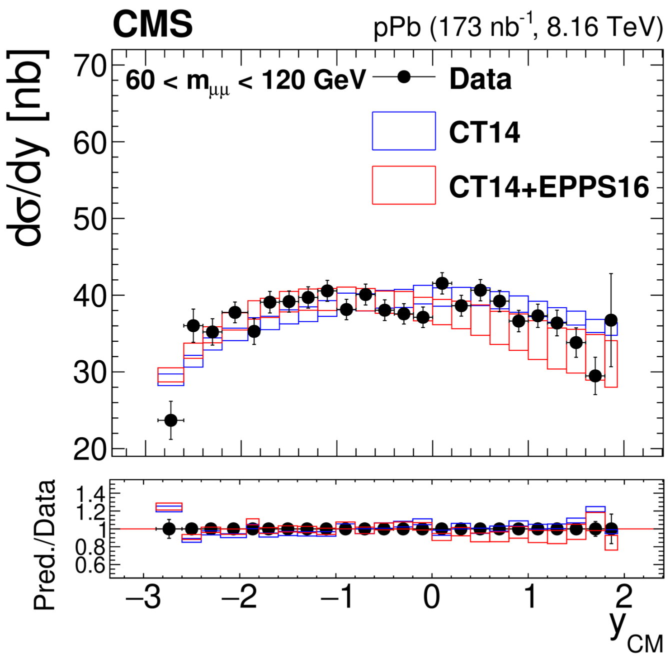

Fiducial (without acceptance correction)

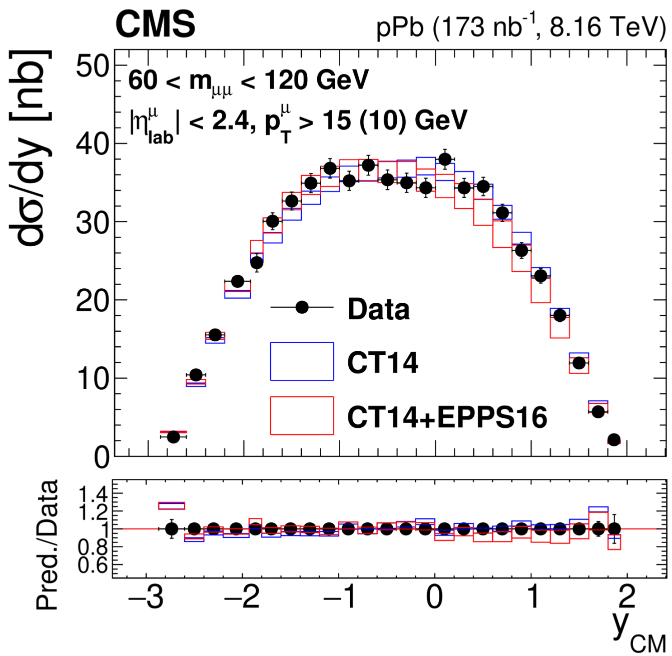

Fiducial measurements : Absence of acceptance correction

→ Lower theoretical uncertainties + Reduction of model dependence

Differential cross sections (1) – mass, y_{CM} dependence

Fiducial (without acceptance correction)

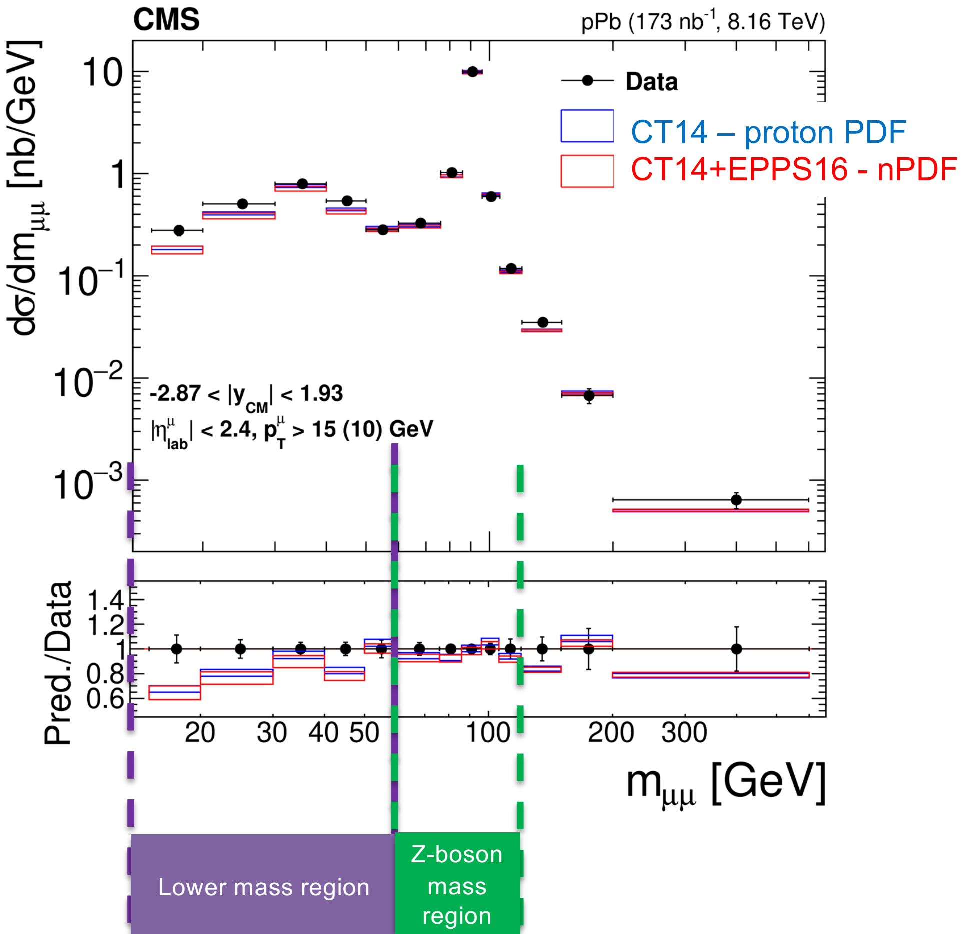

Lower mass region
$15 < m_{\mu\mu} < 60$ GeV

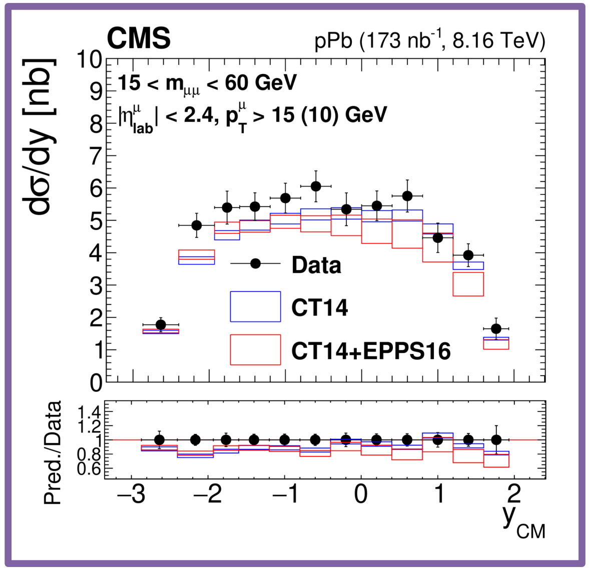

Z-boson mass region
$60 < m_{\mu\mu} < 120$ GeV

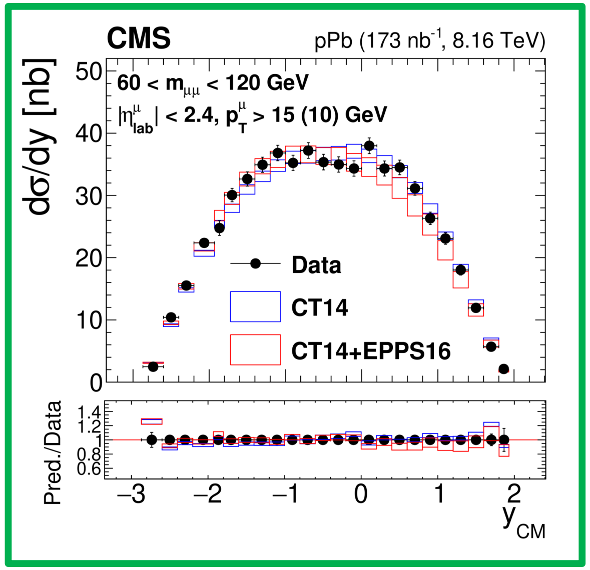

- In lower mass region, we can access to lower x region
- EPPS16 can give better description than CT14 PDF alone, in Z boson mass region
- Uncertainties in the measurement are smaller than nPDF uncertainties, in Z boson mass region

Differential cross sections (2) – p_T, ϕ^* dependence

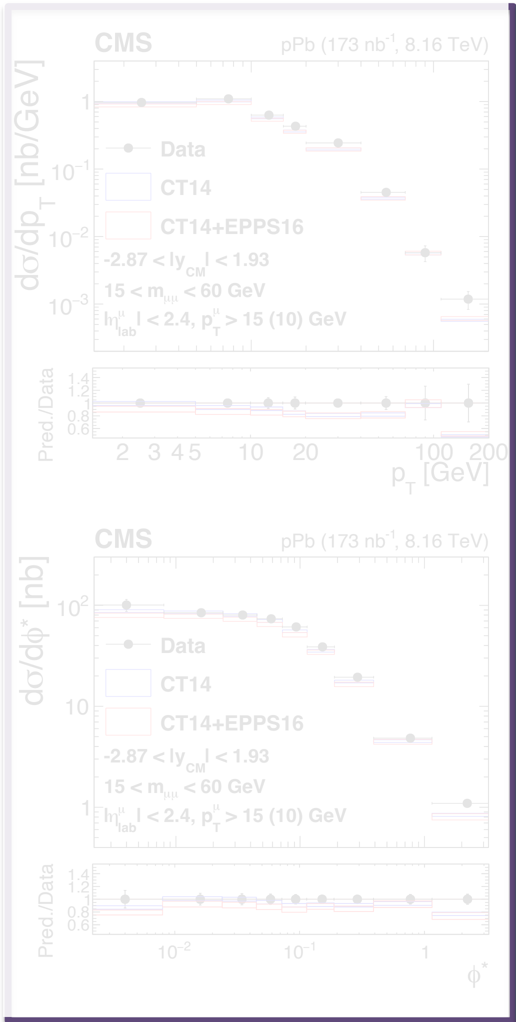

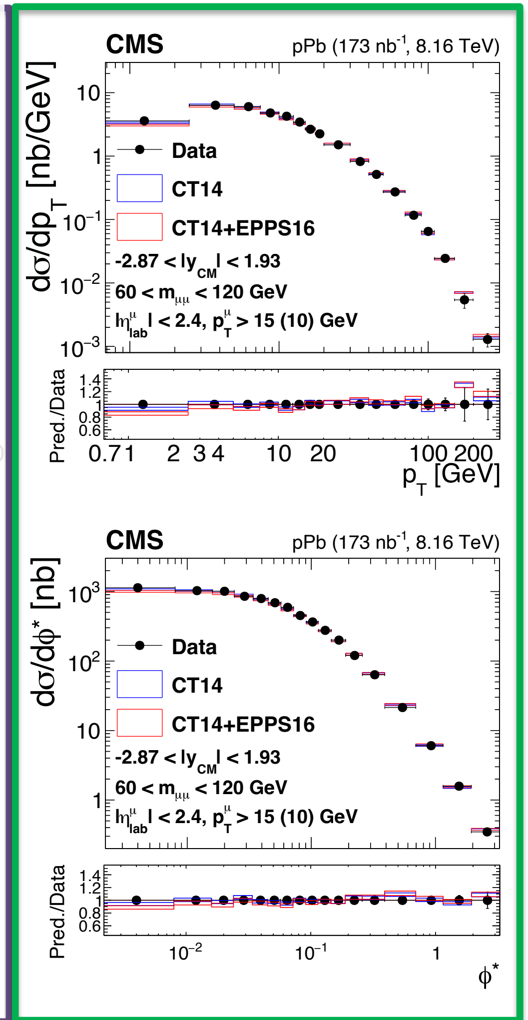

Fiducial (without acceptance correction)

CT14 – proton PDF

CT14+EPPS16 - nPDF

- **From p_T or ϕ^* results in Z boson mass region, CT14 looks give better description, contrary to $|y_{CM}|$ results**
- **Strong conclusions about nPDFs are prevented by imperfect modelling in POWHEG**
- **The precise measurement in pPb collisions provides new insight into the soft QCD phenomena dominating the production at low boson p_T or ϕ^***

Differential cross sections (2) – p_T, ϕ^* dependence

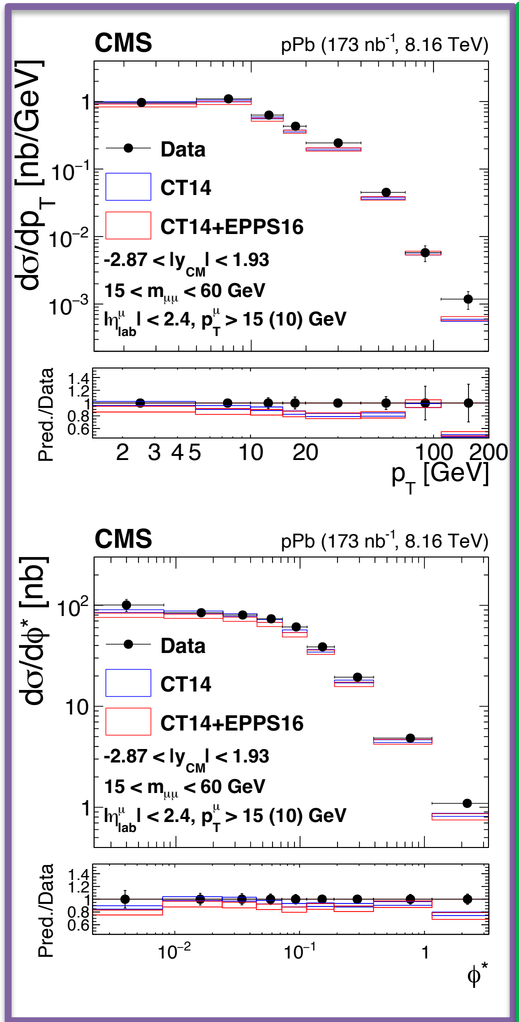

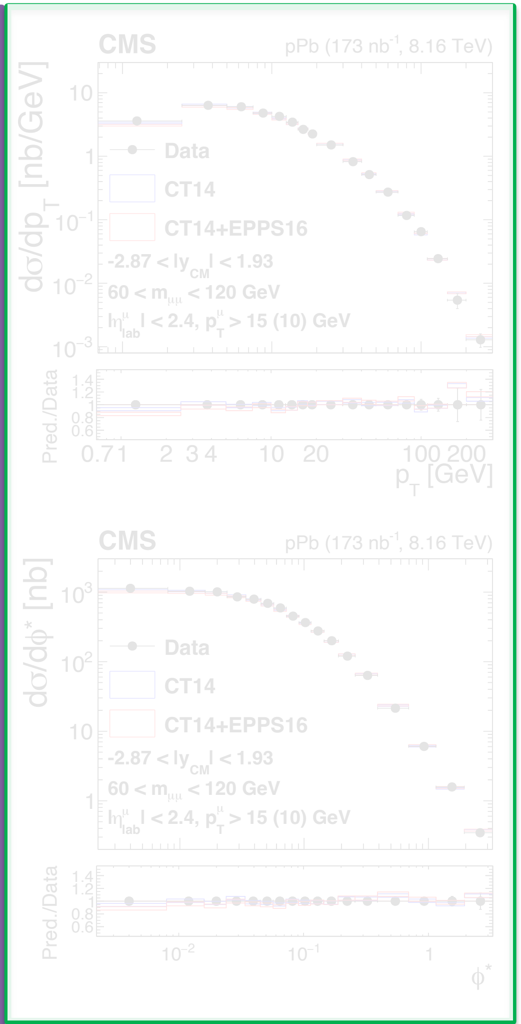

Fiducial (without acceptance correction)

CT14 – proton PDF

CT14+EPPS16 - nPDF

- From p_T or ϕ^* results in Z boson mass region, CT14 looks give better description, contrary to $|y_{CM}|$ results
- Strong conclusions about nPDFs are prevented by imperfect modelling in POWHEG
- **The precise measurement in pPb collisions provides new insight into the soft QCD phenomena dominating the production at low boson p_T or ϕ^***

Forward-backward ratio

p-going
y>0

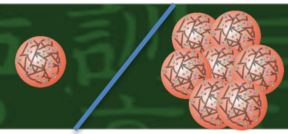

Pb-going
y<0

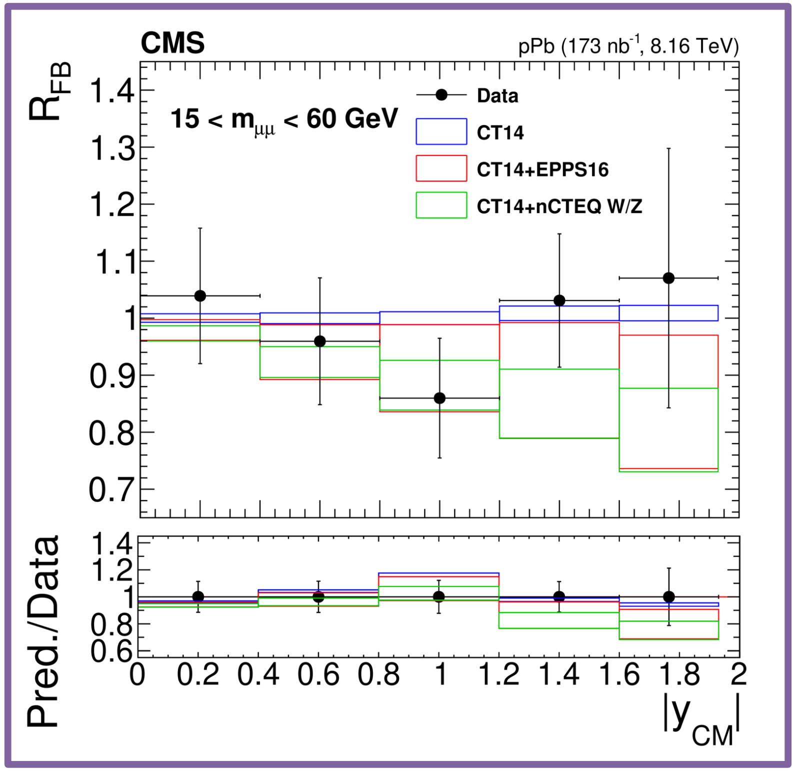

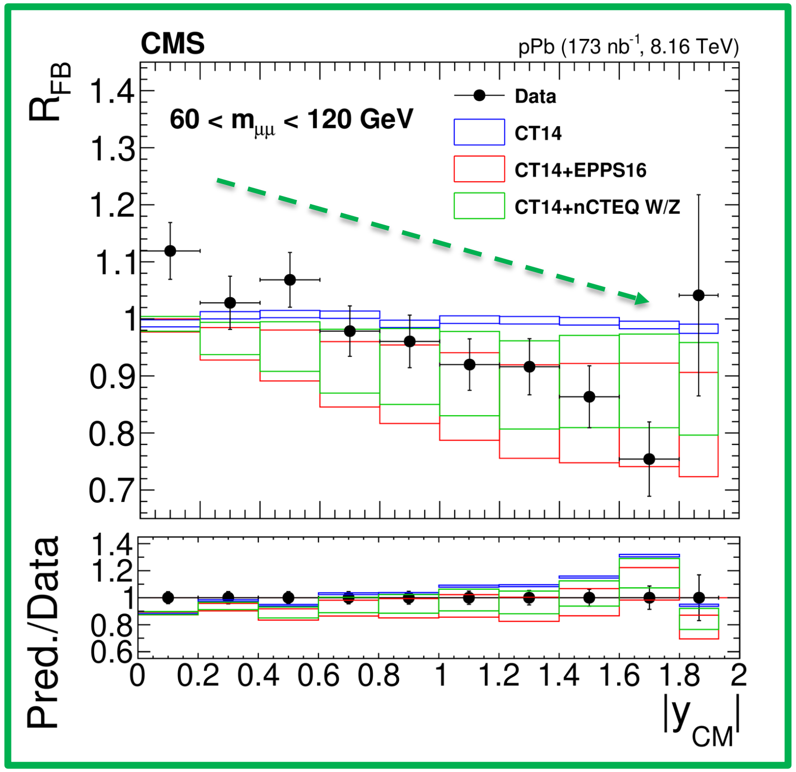

proton PDF
CT14
nPDF
EPPS16
CTEQW/Z

- **Lower uncertainties by partial cancellation the correlated uncertainties**
- **In Z boson mass region, indication of a $R_{FB} < 1$ is found, consistent with the expectations from nPDFs than proton PDF only**
- **Smaller uncertainties of data than the model can give the constraint to further modelling**

DY data is applied in nPDF improvement

nNNPDF3.0

arXiv (2022) 2201.12363

Process	Dataset	Ref.	n_{dat}	Nucl. spec.	Theory
NC DIS	NMC 96	[53]	123/260	^{2}D/p	APFEL
	SLAC 91	[54]	38/211	^{2}D	APFEL
	BCDMS 89	[55]	250/254	^{2}D	APFEL
Fixed-target DY	FNAL E866	[56]	15/15	^{2}D/p	APFEL
	FNAL E605	[57]	85/119	^{64}Cu	APFEL
Collider DY	ALICE $W^{\pm}$, Z (5.02 TeV)	[58]	6/6	^{208}Pb	MCFM
	LHCb Z (5.02 TeV)	[28]	2/2	^{208}Pb	MCFM
	ALICE Z (8.16 TeV)	[60]	2/2	^{208}Pb	MCFM
	CMS Z (8.16 TeV)	[61]	36/36	^{208}Pb	MCFM
Dijet production	CMS p–Pb/pp (5.02 TeV)	[27]	84/84	^{208}Pb	NLOjet++
Prompt photon production	ATLAS p–Pb/pp (8.16 TeV)	[62]	43/43	^{208}Pb	MCFM
Prompt D^0 production	LHCb p–Pb/pp (5.02 TeV)	[28]	37/37	^{208}Pb	POWHEG

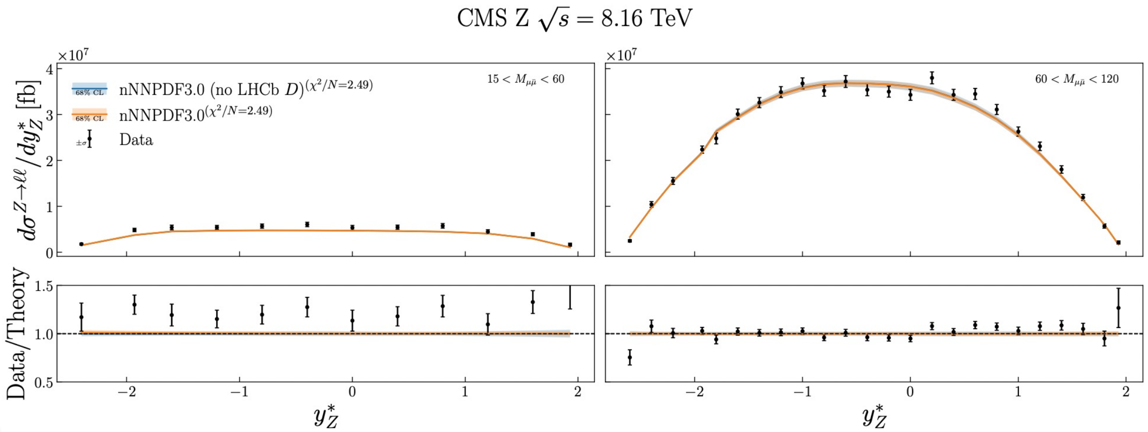

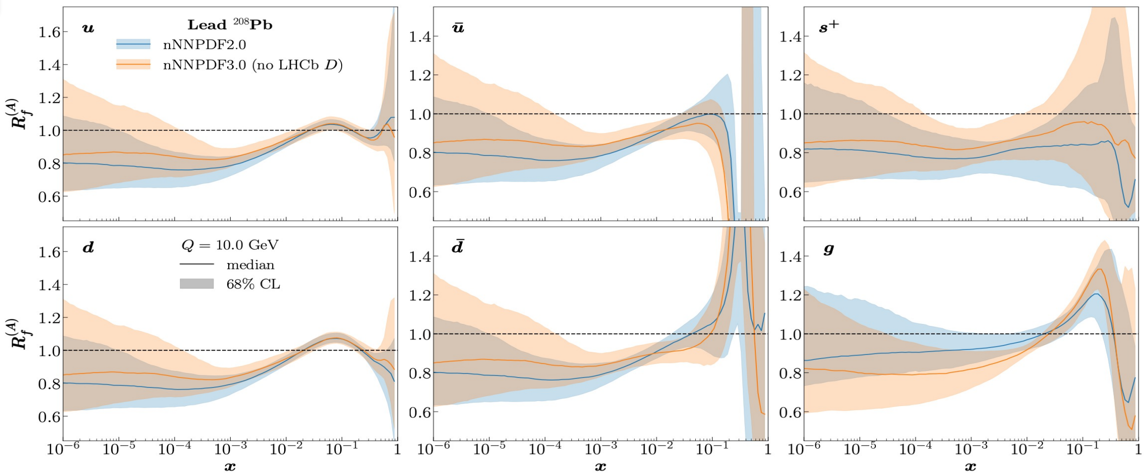

Expect to provide constraints to models and contribute to further developments ☺

Then what is the future of the DY analysis?

- **DY in pPb during the run 2 HI period show the smaller uncertainty than in PDF**
  - But in run 3 period, pPb data will not be provided
- **Only PbPb data in run 3 HI period**
  - Up to run 2 period, data uncertainty is closed to PDF uncertainty
    - Expect the visible smaller uncertainty in run 3 accumulated data
- **DY Analysis in pp collision is continuous with improvement**
  - Leading group is in Korean (close to ATHIC range)
- **DY in PbPb might show the nPDF effect clearly than in pPb**

- **Still might be difficult, but might not be impossible**

run period	year	Collision energy	integrated luminosity (μb^{-1})
run 2	2015	5.02	594.6
	2018		1893.4
run 3	2023	5.36	1979.7
	2024		1668.3
	2025		?
	2026		?

Expect 4 times than in 2018?

Summary

- **Drell-Yan (DY) process is the powerful probe to investigate the inside of the nucleus, but only focused to Z boson region until now**
- **In first Drell-Yan measurement results (lower mass + Z boson mass(ϕ*)) at proton-ion collisions**
  - Drell-Yan results for $60 < m_{\mu\mu} < 120$ GeV have smaller uncertainties than those from models, expect to provide novel constraints on nPDFs
  - Measurements for $15 < m_{\mu\mu} < 60$ GeV give access to a new phase space for nPDF studies
- **In run 3 period, expect more accurate measurement with larger statistics**

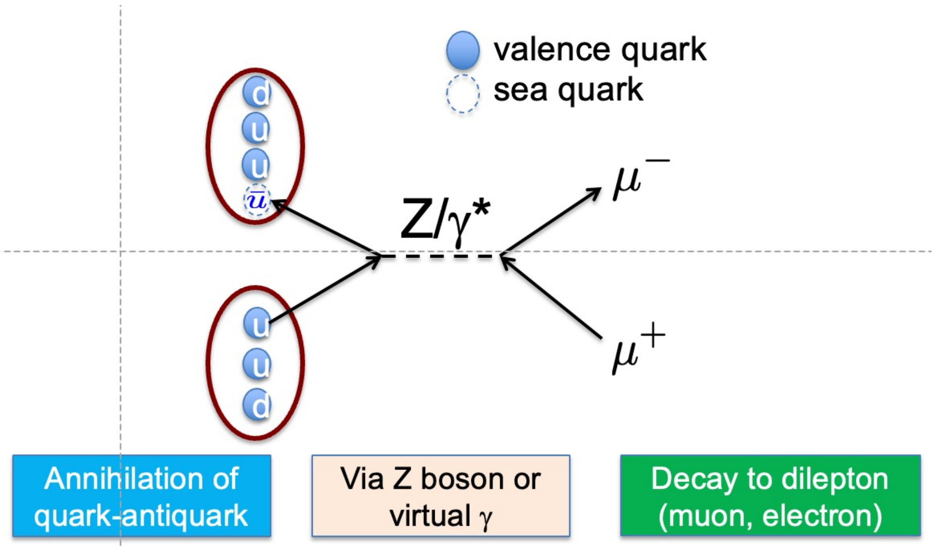

Lower mass region

Z-boson mass region

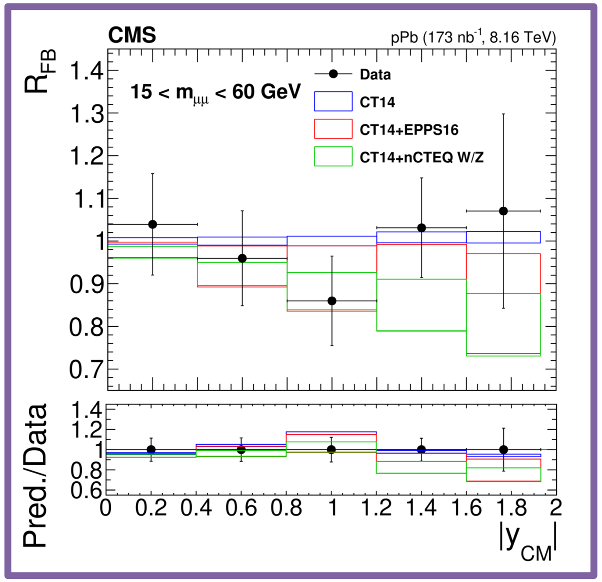

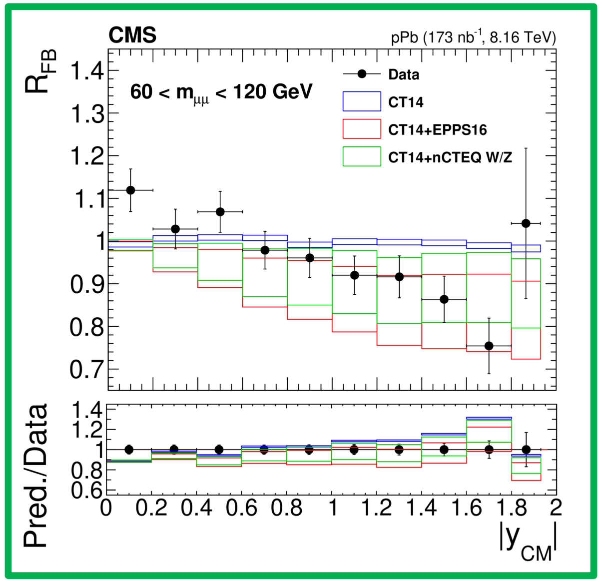

Summary

- **Drell-Yan (DY) process is the powerful probe to investigate the inside of the nucleus, but only focused to Z boson region until now**
- **In first Drell-Yan measurement results (lower mass + Z boson mass(ϕ^*)) at proton-ion collisions**
  - Drell-Yan results for $60 < m_{\mu\mu} < 120$ GeV have smaller uncertainties than those from models, expect to provide novel constraints on nPDFs
  - Measurements for $15 < m_{\mu\mu} < 60$ GeV give access to a new phase space for nPDF studies
- **In run 3 period, expect more accurate measurement with larger statistics**

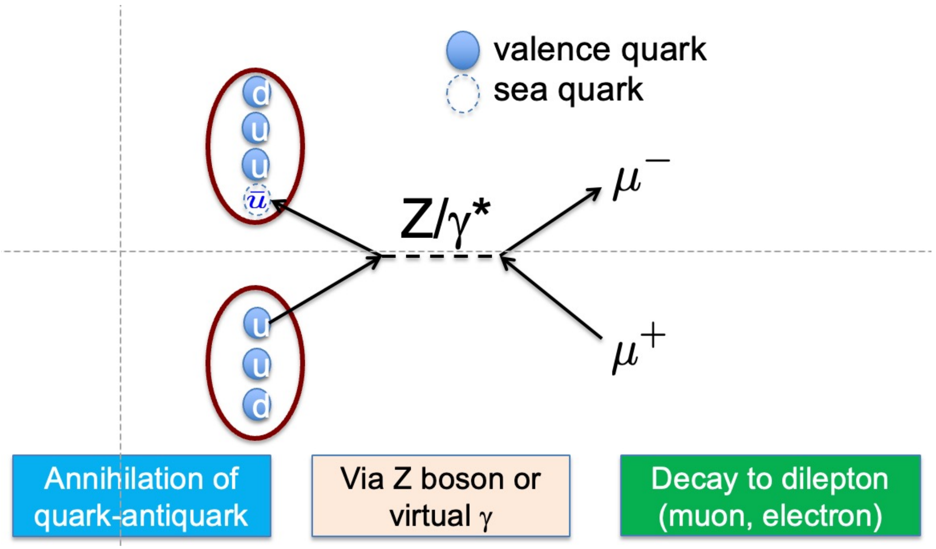

Lower mass region

Z-boson mass region

Hope to see DY in PbPb collision results here..

Thank you very much for your attention
Hope a **D**elightful **Y**ear for you

Kinematic coverage

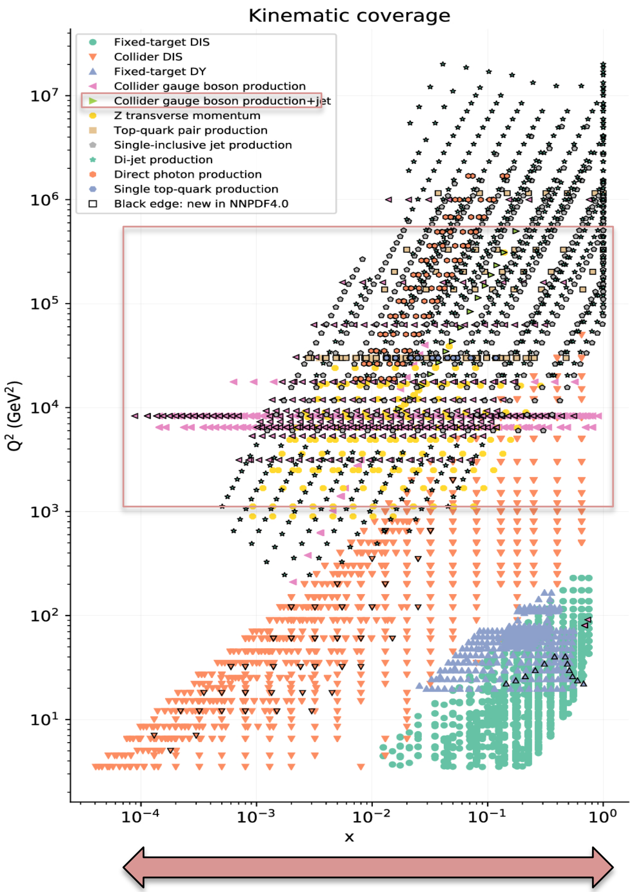

$$x = \frac{Q}{\sqrt{s_{\mathrm{NN}}}} e^{y_{\mathrm{CM}}}$$

- **x : momentum fraction**
- **Q : dimuon mass**
- $\sqrt{s_{NN}}$: collision energy
- y_{CM} : dimuon's rapidity in center-of-mass frame

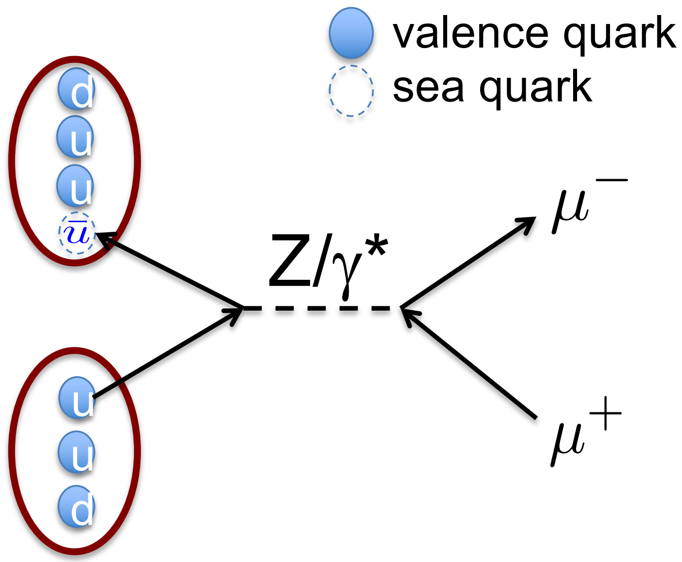

Annihilation of quark-antiquark

Via Z boson or virtual γ

Decay to dilepton (muon, electron)

nPDF region explanation

1. Shadowing Region ($x \lesssim 0.1$):

- **Meaning:** In this region, the parton densities in a nucleus are suppressed compared to the sum of the parton densities of individual nucleons. This effect is attributed to coherent interactions between partons in different nucleons within the nucleus.
- **Trend:** The nuclear modification ratio $R_A(x, Q^2) = \frac{f_A(x,Q^2)}{A f_N(x,Q^2)}$ (where f_A is the nuclear PDF, f_N is the nucleon PDF, and A is the atomic mass number) is less than 1, showing a suppression of partons, particularly gluons and sea quarks.
- **Physical Explanation:**
  - Coherence effects, such as multiple scattering of partons and gluon recombination (saturation effects), reduce the effective number of partons.
  - Strong in heavy nuclei due to the dense partonic environment.

2. Anti-Shadowing Region ($0.1 \lesssim x \lesssim 0.3$):

- **Meaning:** Here, the nuclear parton densities are enhanced relative to the free nucleon case.
- **Trend:** $R_A(x, Q^2) > 1$, showing an excess of partons in this range.
- **Physical Explanation:**
  - This enhancement is often linked to momentum conservation and the interplay between nuclear effects like gluon exchange or the redistribution of partons from shadowed regions.
  - Anti-shadowing is more pronounced in quark distributions than gluons.

3. EMC Region ($0.3 \lesssim x \lesssim 0.8$):

- **Meaning:** The EMC (European Muon Collaboration) effect refers to a significant suppression of parton densities in the intermediate-x region for nuclei compared to free nucleons.
- **Trend:** $R_A(x, Q^2) < 1$ in this region, with a gradual dip.
- **Physical Explanation:**
  - The origin of the EMC effect is not fully understood, but possible explanations include:
    - Modifications of the nucleon structure due to the nuclear medium.
    - Nucleon-nucleon correlations (e.g., short-range correlations).
    - Mesonic degrees of freedom or binding effects.

4. Fermi Motion Region ($x \gtrsim 0.8$):

- **Meaning:** At high x, partons are influenced by the Fermi motion of nucleons within the nucleus.
- **Trend:** $R_A(x, Q^2) > 1$, with a steep rise due to the high-momentum tail of partons.
- **Physical Explanation:**
  - This region is dominated by the effects of the nucleons' intrinsic motion within the nucleus, leading to an enhancement of parton densities at high x.

Help from chatGPT ☺

Table 1: Key features of recent global analyses of nuclear PDFs.

Analysis	nCTEQ15HQ (50)	EPPS21 (51)	nNNPDF3.0 (52)	TUJU21 (80)	KSASG20 (81)
Theoretical input:					
Perturbative order	NLO	NLO	NLO	NNLO	NNLO
Heavy-quark scheme	SACOT$-\chi$	SACOT$-\chi$	FONLL	FONLL	FONLL
Value of $\alpha_s(M_Z)$	0.118	0.118	0.118	0.118	0.118
Charm mass m_c	1.3 GeV	1.3 GeV	1.51 GeV	1.43 GeV	1.3 GeV
Bottom mass m_b	4.5 GeV	4.75 GeV	4.92 GeV	4.5 GeV	4.75 GeV
Input scale Q_0	1.3 GeV	1.3 GeV	1.0 GeV	1.3 GeV	1.3 GeV
Data points	1484	2077	2188	2410	4353
Independent flavors	5	6	6	4	3
Parameterization	Analytic	Analytic	Neural network	Analytic	Analytic
Free parameters	19	24	256	16	18
Error analysis	Hessian	Hessian	Monte Carlo	Hessian	Hessian
Tolerance	$\Delta\chi^2 = 35$	$\Delta\chi^2 = 33$	N/A	$\Delta\chi^2 = 50$	$\Delta\chi^2 = 20$
Proton PDF	~CTEQ6.1	CT18A	~NNPDF4.0	~HERAPDF2.0	CT18
Proton PDF correlations		✓	✓		
Deuteron corrections	(✓)[a,b]	✓[c]	✓	✓	✓
Fixed-target data:					
SLAC/EMC/NMC NC DIS	✓	✓	✓	✓	✓
– Cut on Q^2	4 GeV^2	1.69 GeV^2	3.5 GeV^2	3.5 GeV^2	1.2 GeV^2
– Cut on W^2	12.25 GeV^2	3.24 GeV^2	12.5 GeV^2	12.0 GeV^2	
JLab NC DIS	(✓)[a]	✓			✓
CHORUS/CDHSW CC DIS	(✓/-)[b]	✓/-	✓/-	✓/✓	✓/✓
NuTeV/CCFR 2μ CC DIS	(✓/✓)[b]		✓/-		
pA DY	✓	✓	✓		✓
πA DY		✓			
Collider data:					
Z bosons	✓	✓	✓	✓	
$W^\pm$ bosons	✓	✓	✓	✓	
Light hadrons	✓	✓[d]			
– Cut on p_T	3 GeV	3 GeV			
Jets		✓	✓		
Prompt photons			✓		
Prompt D^0	✓	✓	✓[e]		
– Cut on p_T	3 GeV	3 GeV	0 GeV		
Quarkonia (J/ψ, ψ', Υ)	✓				

[a] nCTEQ15HIX (26); [b] nCTEQ15ν (114); [c] through CT18A; [d] only π^0 in DAu; [e] only forward ($y > 0$).

Previous Z boson measurement – measured variables

- **Differential cross section**
  - vs. p_T, y, and <N_{part}> (centrality)
  - With larger statistics, finer binning is available

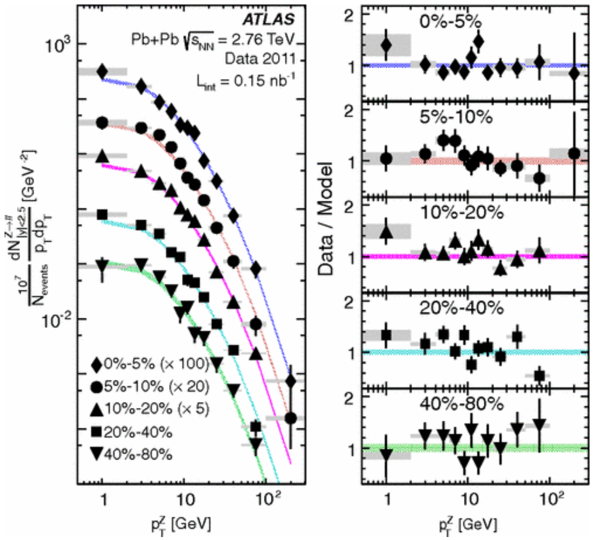

ATLAS : PRL 110 (2013) 022301

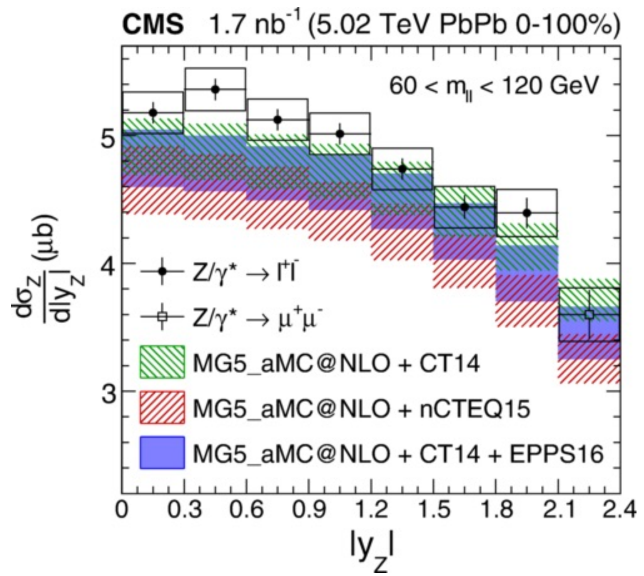

CMS : PRL 127 (2021) 102002

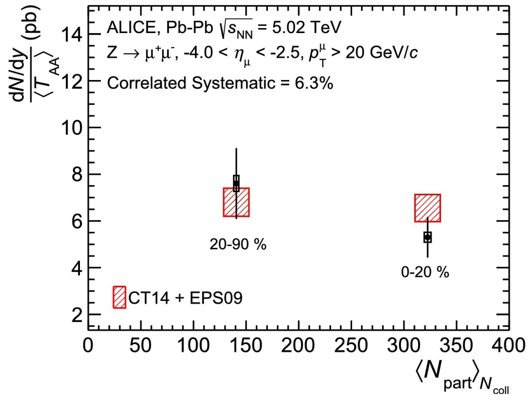

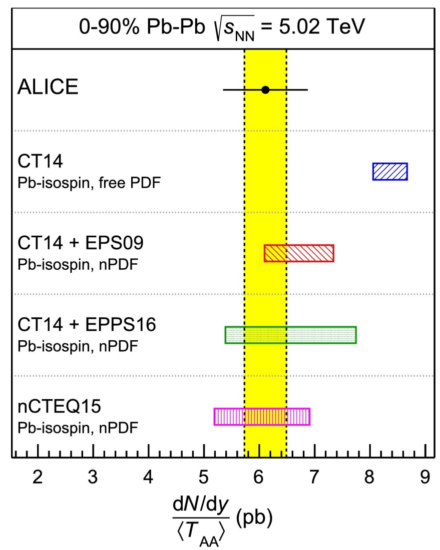

ALICE : PLB 780 (2018) 372

T_{AA}-normalized Z boson yields in PbPb

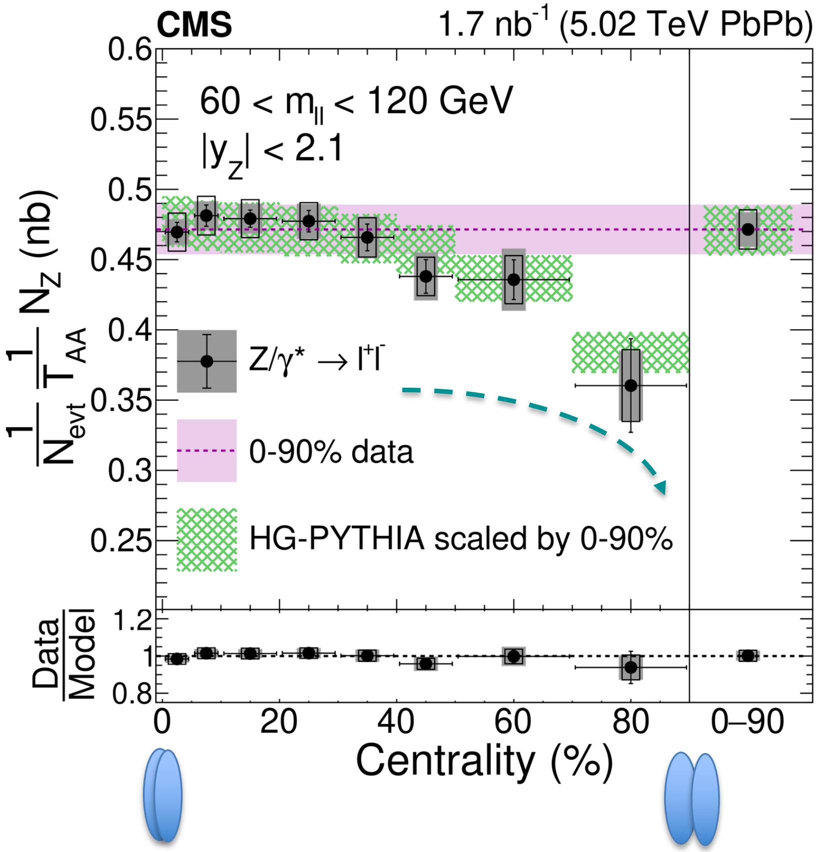

PRL 127 (2021) 102002

- **T_{AA} : transverse overlap function representing the collision's effective integrated nucleon-nucleon luminosity**

HG-PYTHIA
- PYTHIA particle production +. HIJING initial collision geometry
- Describe geometric and selection biases

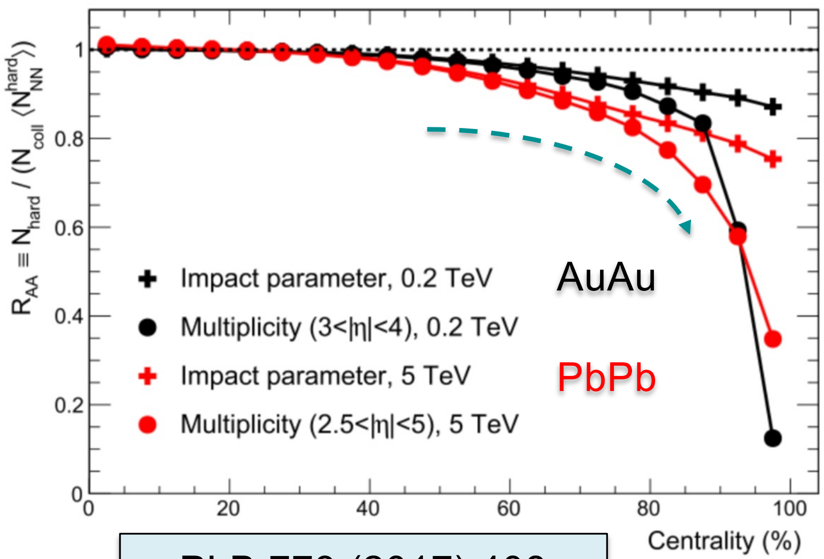

PLB 773 (2017) 408

Previous Z boson measurement – measured variables

- R_{AA}, R_{pPb} : Ion collision compared to pp collision
- Compared with W boson ($R_{W/Z}$)

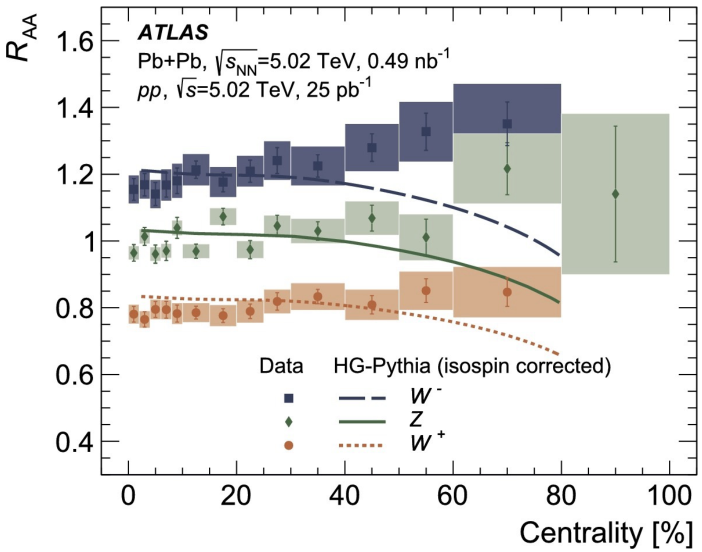

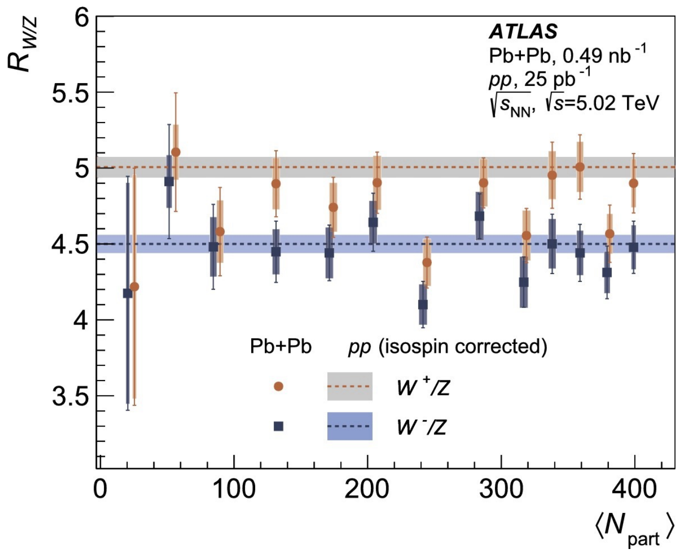

ATLAS : PLB 802 (2020) 135262

- Azimuthal anisotropy (v_2)
  - Zero as expected

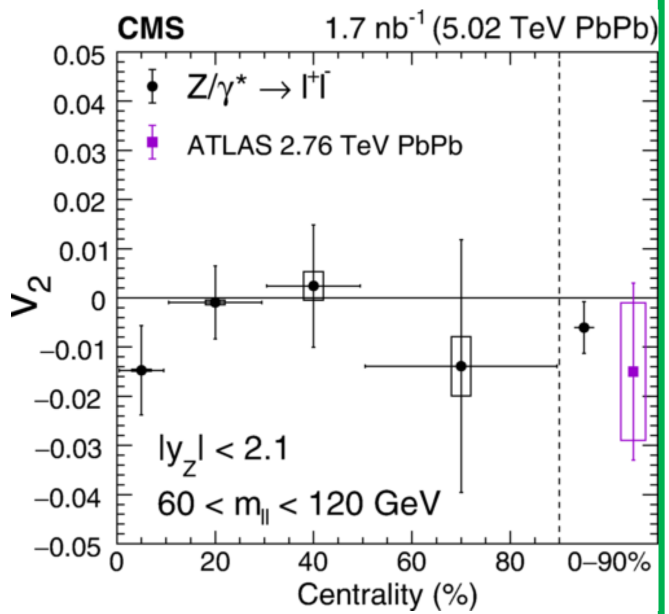

CMS : PRL 127 (2021) 102002

eμ data-driven method

- **If we believe MC totally,**
  – But we can't, validate with other kind of data

$$N_{Bkg.}^{Est.} = \frac{N_{Bkg.}^{MC}}{N_{Total}^{MC}} * N_{All}^{Data}$$

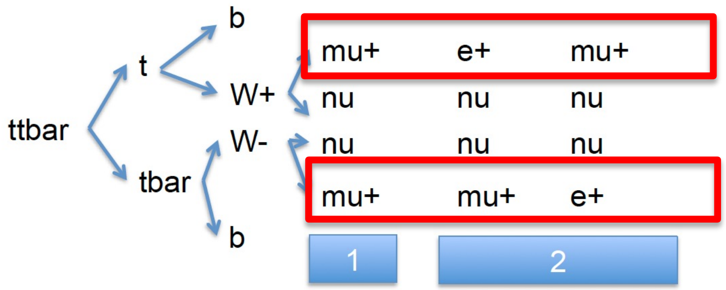

$$N_{Bkg.}^{Est.\mu\mu} = \frac{N_{Bkg.}^{MC,\ \mu\mu}}{N_{Bkg.}^{MC,\ e\mu}} * N_{Bkg}^{Data(Obs.)\ e\mu}$$

$$N_{Bkg.}^{Est.\ \mu\mu} = \frac{N_{Bkg.}^{MC,\ \mu\mu}}{N_{Bkg.}^{MC,\ e\mu}} * \frac{N_{Bkg.}^{MC,\ e\mu}}{N_{Total.}^{MC,\ e\mu}} * N_{All}^{Data(Obs.)\ e\mu}$$

$$N_{Bkg.}^{Est.\ \mu\mu} = \frac{N_{Bkg.}^{MC,\ \mu\mu}}{N_{Total.}^{MC,\ e\mu}} * N_{All}^{Data(Obs.)\ e\mu}$$

  – Validate with eμ data

Fake rate(misidentification) method

- **Background with one (W+jet) or two (QCD multijet)muon inside jets and identified as prompt muon**
  – Also pass the muon selection including muon ID and isolation cuts

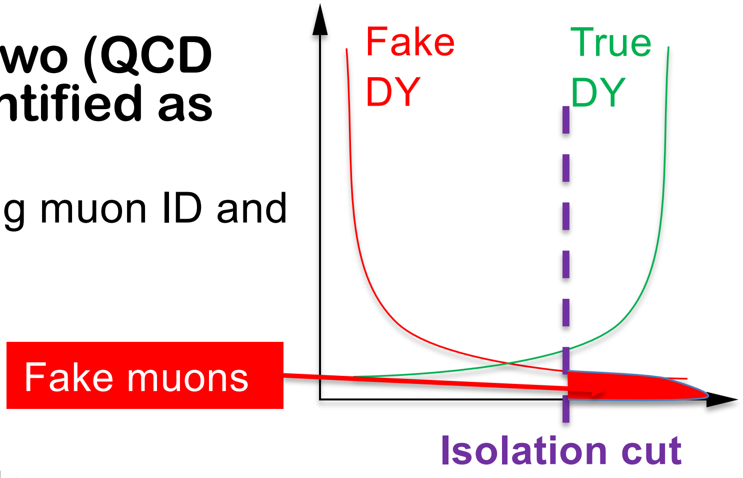

- **Use "fake rate" technique**
  – Using QCD or W+jet MC, get fake rate

$$\text{Fake rate (FR)} = \frac{\text{Muons passing all selection cuts}}{\text{Muons passing all selection cuts w/o isolation}} = \frac{\text{iso}}{\text{tight}}$$

  - # of fake muons = # of total muons * FR
  - # of non-fake muons = # of total muons * (1-FR)

  – # of fake muons = FR /(1-FR) * # of non-fake muons

- **Validate with same sign data with other analysis cuts**

Forward-backward ratio

p-going
y>0

Pb-going
y<0

W boson in pPb

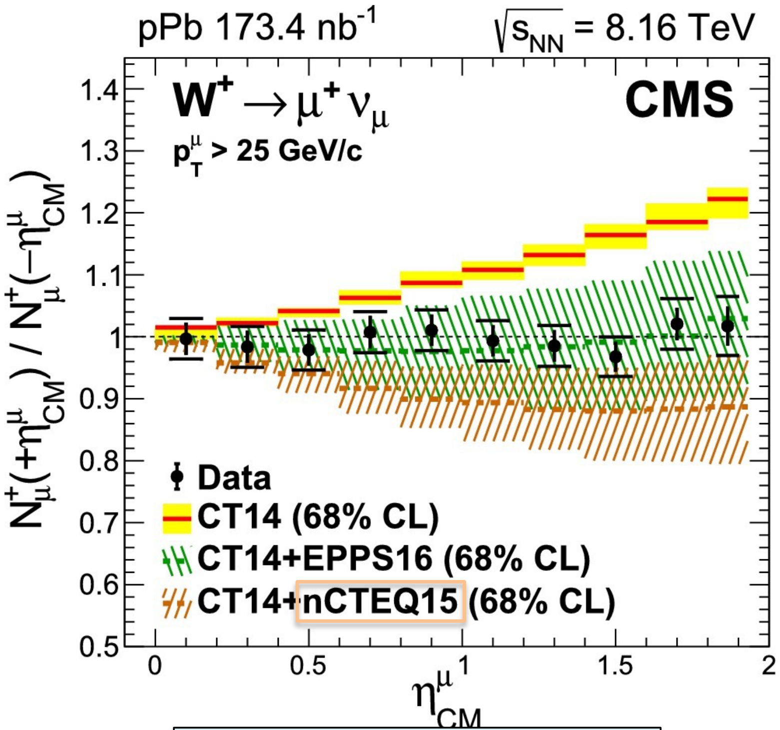

PLB 800 (2020) 135048

Drell-Yan in pPb

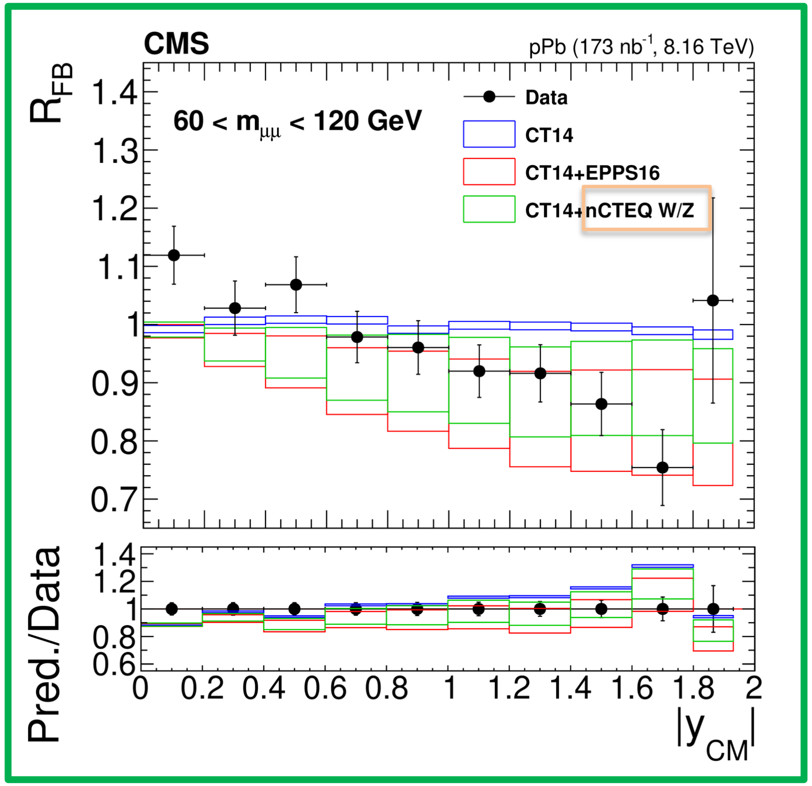

- For both cases, deviation from free proton PDF(CT14) is observed
- Shadowing in nCTEQ15, hinted by the W boson measurement, is not predicted with nCTEQ15WZ

Z bosons in pPb (CMS)

Z boson in pPb 5.02 TeV (2013)

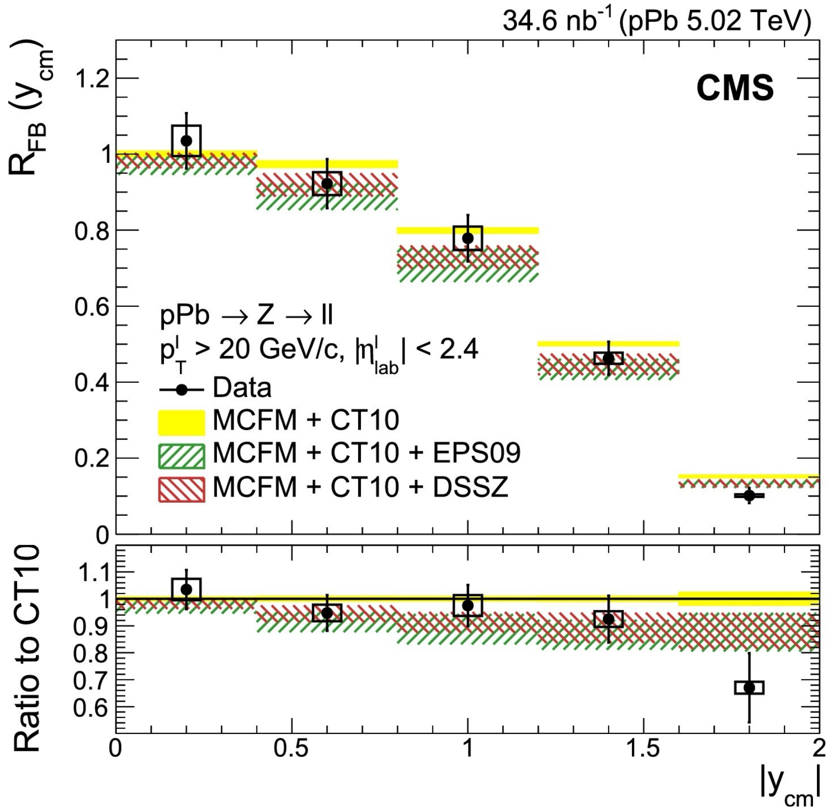

Drell-Yan in pPb 8.16 TeV (2016)

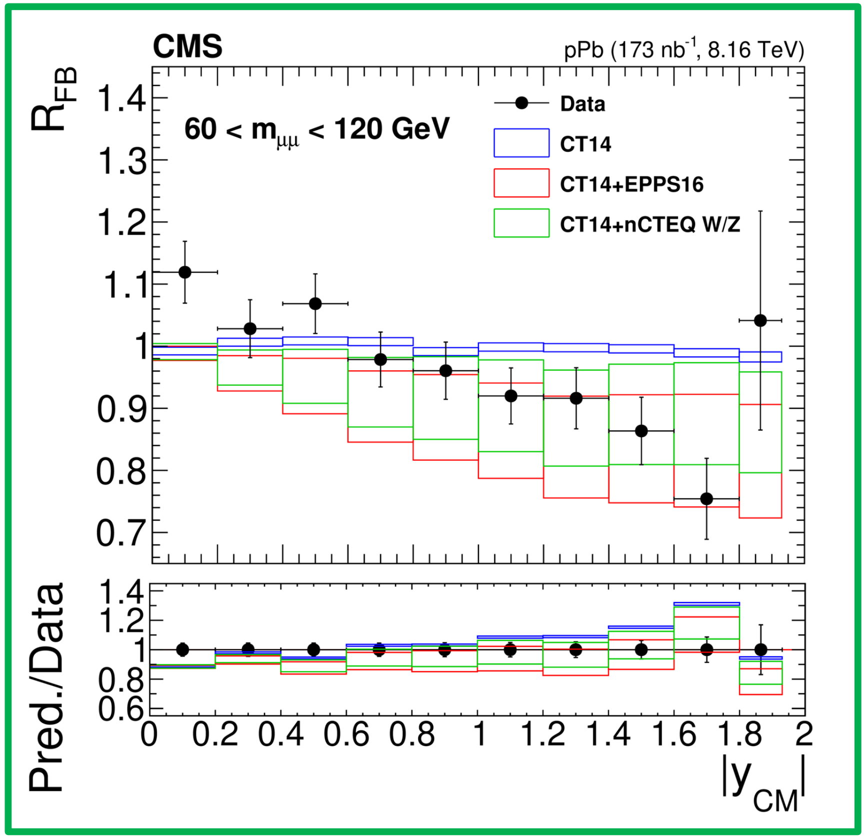

PLB 759 (2016) 36

Favor nPDF than proton PDF only

Correlation between p_T vs. ϕ^*

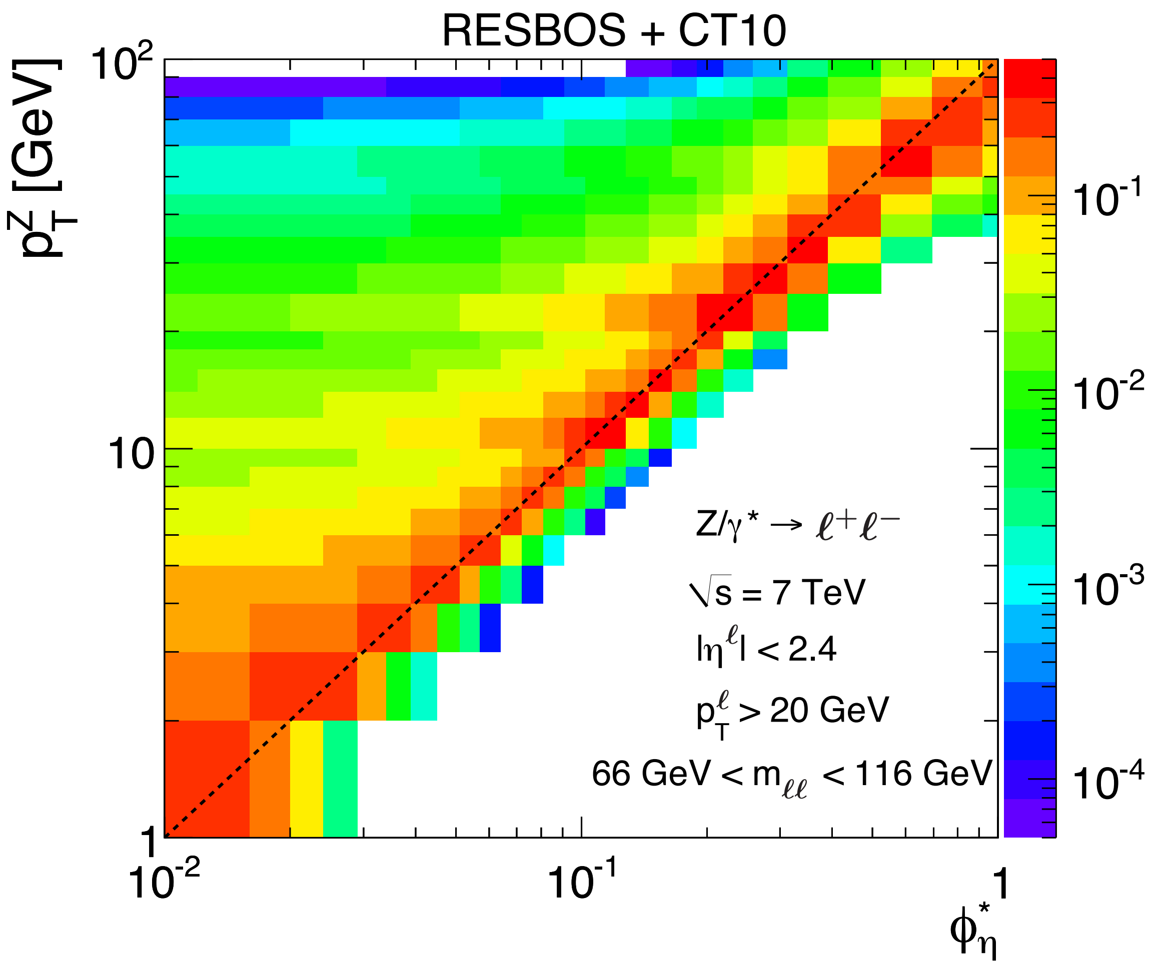

PLB 720 (2013) 32

Summary of systematic uncertainties

Source of uncertainty	15 < $m_{\mu\mu}$ < 60 GeV	60 < $m_{\mu\mu}$ <120 GeV	Correlated
Event activity reweighting	< 3%	< 1%	Fully correlated
Muon momentum	< 1%	< 3%	
Data-driven efficiencies	1-5%	1-4%	
Acceptance and efficiency (MC stat.)	< 4%	< 4%	
Background estimation	2-15%	0.1-3%	Fully correlated
Acceptance and efficiency (theory)	1-10% (< 1%)	< 1% (< 1%)	
Unfolding: detector resolution	< 2%	< 2%	Fully correlated
Unfolding : FSR	< 1%	< 1%	Fully correlated
Total	6-15%	1-12%	

Correlation matrices for the systematic uncertainties

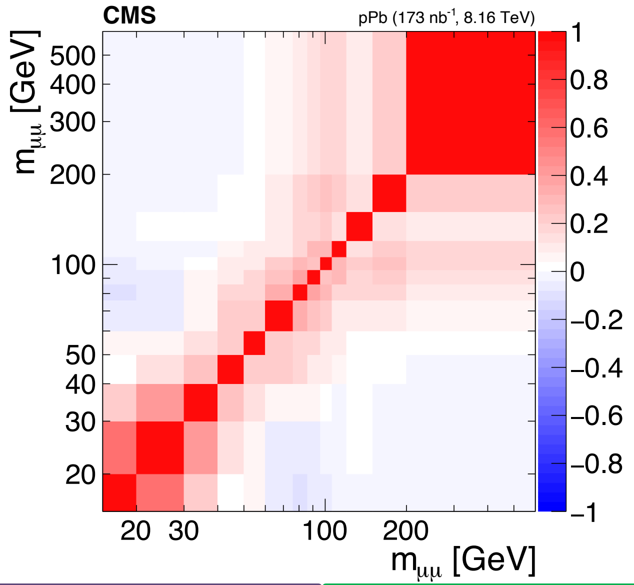

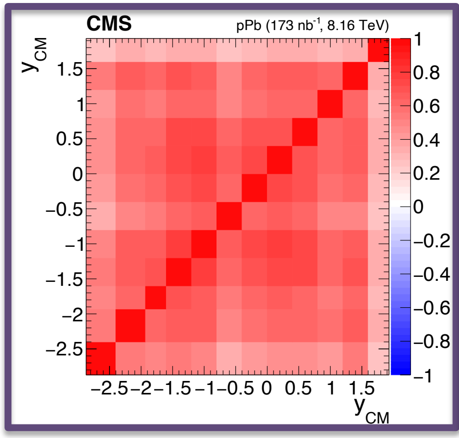

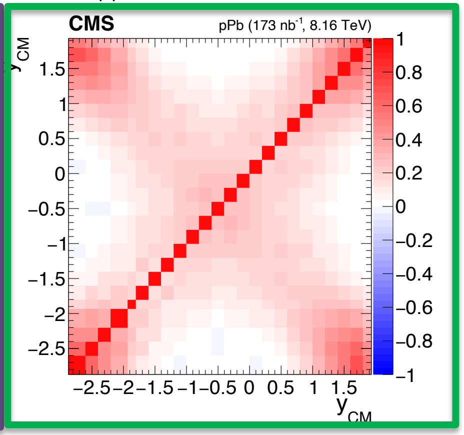

- **Correlation across bins of all the systematic uncertainties have also been evaluated**
- **Integrated luminosity is excluded for clarity**
- **The difference between the matrices in the two mass selections can be explained by the background uncertainty, which is one of the dominant systematics source**